Rapid, simultaneous increases in the effective sizes of adaptively divergent yellow perch (*Perca flavescens*) populations

Running title: Rapid parallel increases in *Ne*

Abstract

Aquatic ecosystems are highly dynamic environments vulnerable to a wide variety of natural and anthropogenic disturbances. High-economic value fisheries are one of many ecosystem services affected by these disturbances and it is critical to accurately characterize their genetic diversity and effective population sizes through time. We used genome-wide data to reconstruct the demographic histories of economically important yellow perch (*Perca flavescens*) populations. In two isolated and genetically divergent populations, we provide strong evidence for simultaneous increases in effective population sizes over both historic and contemporary time scales including negative genome-wide estimates of Tajima's D, 3.1 times more SNPs than adjacent populations, and effective population sizes that have increased 10- and 47-fold from their minimum. We also identified parallel, genetic adaptation to reduced visual clarity in the same two habitats. These results suggest that the synchrony of key ecological and evolutionary processes can drive parallel demographic and evolutionary trajectories across independent populations.

Keywords: demographic history, effective population size, fisheries, genomics, parallel evolution

Background

Accurate estimates of effective population sizes (*Ne*) are critical for the successful management and conservation of threatened and endangered species. The concept of *Ne* was first introduced in 1931, and often refers to the size of an idealized population with constant size and random mating that experiences an equivalent rate of genetic drift as the population under study(1). Consequently, estimates of effective population size tend to be orders of magnitude smaller than estimates of census population sizes(2–12). From a conservation and management perspective, effective population size matters in several key aspects: 1.) *Ne* is a major determinant of nucleotide variation (*i.e.*, $4Ne\mu$ under a neutral model), 2.) *Ne* provides an estimate of overall level of standing genetic variation within a population that can respond to ongoing and future selective events (*e.g.*, climate change) and provides a unified frame of reference for comparisons across species or populations, and 3.) estimates of *Ne* for various genomic regions can shed light on the different evolutionary processes and histories that have shaped genetic variation across the genome(4). Thus, changes in effective population sizes through time can provide information on how populations are responding to novel stressors, such as climate change(13–16), changes in food web dynamics(17), habit alteration and destruction(14,17), and overexploitation(9,13–15,18).

Accurate estimates of effective population sizes are particularly needed in fisheries to guide sustainable harvest practices in economically important populations. *Ne* is a critical metric for the successful assessment and management of fisheries stocks as it not only provides a fisheries-independent approach, avoiding the biases inherent in some field- or catch-based methods(19), but also reflects the adaptative potential of different stocks under constantly changing environments(19,20). Estimates of effective population sizes can even forecast

overharvest and potential collapses in commercial fisheries, as signaled by either substantial reductions in effective population sizes or declining ratios of effective to census population sizes(6,21,22). Nevertheless, several challenges remain for estimating effective population sizes in fish and fisheries. Estimates of *Ne* often include infinity when the signal for genetic variation arising from genetic drift cannot be estimated with high precision and is instead overwhelmed by noise arising from sampling error(23,24). Also, fish populations are often highly connected due to extensive larval dispersal and juvenile or adult migration(25–28). Such migration and subsequent gene flow can bias, or at the very least complicate estimates of *Ne*(4,29,30). Additional challenges include overlapping generations(29–31), genomic architecture(29), rare alleles(29), sample sizes(29,30), sampling design(29), and sequencing or genotyping errors(29). With advances in high throughput sequencing and the influx of genomic data, many methods(32–36) have been developed to more accurately infer temporal changes in effective population sizes for various data types, including polymorphic sites, short sequence blocks, and whole genome data(4). Empirical assessments of *Ne* using both older and newer methods have mostly demonstrated reductions in effective population sizes over contemporary time scales(8,9,13–18,37–39).

Contemporary increases in effective population sizes, although rarely documented(10,39,40), can occur via one of three mechanisms. First, a reduction in the variance in reproductive success, for example by equalizing mating success throughout a single generation, can result in larger effective population sizes in the next generation(41,42), as demonstrated in captive breeding programs where equalization of full-sib family sizes is often recommended to boost effective population sizes(43–46). Second, introgression from neighboring, genetically divergent populations may generate biases in estimating *Ne*, the

direction of which is determined by the magnitude and continuity of gene flow(29,30). Third, large, consistent increases in adult abundance within a population, perhaps due to improved environmental conditions and management policies, can also cause increases in effective population sizes(40). These last two mechanisms may also be accompanied by several other genetic indicators for recent population expansions, including negative values of Tajima's D, shifts in site frequency spectra, and larger numbers of polymorphic loci with low minor allele frequency(4).

Here, we document large, parallel, and rapid increases in effective population sizes in two yellow perch (*Perca flavescens*) populations separated by more than 350 km. We sequenced the complete genomes and reconstructed the demographic histories for 210 yellow perch collected from five sample sites located throughout the 4,900 cubic km main basin of Lake Michigan and two widely separated sites directly connected to the main basin: Green Bay and Muskegon Lake (Fig. 1a). Historically, yellow perch supported large commercial and recreational fisheries throughout the Great Lakes(47,48), with the maximum annual commercial harvest in Lake Michigan alone reaching 2.6 million kg in 1964(47), but sustained population declines led to closures of commercial fisheries throughout many regions of the Great Lakes in the late 1980s(49). Here, using genome-wide data, we find that the effective population sizes of yellow perch in Green Bay and Muskegon Lake have increased 10- and 47-fold, respectively, from their minimum in the past 5-10 decades. We also find additional genomic signatures associated with older population expansions in these two populations, including negative values of Tajima's D across the genome and an excess of single nucleotide polymorphisms (SNPs) with rare alleles. Lastly, we find signatures of parallel, genetic adaptation to reduced visual clarity in the same two sites that experienced historic and contemporary increases in effective population sizes.

Methods

Data collection

We sampled 210 adult yellow perch from seven locations in Lake Michigan (Green Bay, Muskegon Lake, Grand Haven, Michigan City, Milwaukee, Naubinway, Sutton's Bay; Fig. 1a, Supplementary Table 1) in 2016, 2018 or 2019 using fyke netting, nighttime boat electrofishing, bottom trawls, gill netting and creel surveys, and conducted whole-genome resequencing at a depth of 12.50× (ranging from 5.93× to 18.58×; see "Whole-genome sequencing" in Supplementary Materials for details). We called SNPs following the "Germline short variant discovery (SNPs + Indels)" pipeline provided by the Genome Analysis Toolkit 4.1.9.0 (GATK 4.1.9.0)(50) (see "Variant calling and filtering" in Supplementary Materials for details). We filtered SNPs by minor allele frequency (MAF) in two ways to create two data sets of SNPs suitable for different analyses (Supplementary Table 3): a study-wide data set and a within-group data set (see details in "Variant calling and filtering" in Supplementary Materials). Study-wide MAF filtering is useful for delineating populations, while within-group filtering is essential for identifying rare variants within each population. Thus, for population structure analyses, we used the study-wide data set, whereas we used the within-group data sets for all subsequent analyses (Supplementary Table 3).

Population structure analysis

To infer the phylogenetic relationship among the seven sample sites, we constructed phylogenetic trees using 5,000 randomly selected SNPs. We first converted SNPs in VCF format into PHYLIP format and then constructed a phylogenetic tree using RAxML version 8.2.12(51). When running RAxML, we selected the GTRGAMMA model, set the random number seed for parsimony inferences to 12345 and the number of alternative runs on distinct starting trees to

1000, turned on rapid bootstrapping, ran rapid bootstrap analysis, and searched for the best-scoring ML tree in each run. We viewed the phylogenetic tree using MEGA11(52). To further investigate the population structure, we first conducted principal coordinate analysis on all individuals with 50,000 randomly selected SNPs in *hierfstat* in R 4.2.1(53). Next, we conducted principal coordinate analysis with pairwise F_{ST} using GenAlEx 6.51b2(54). Weir and Cockerham's F_{ST} was calculated for each pair of sample sites using VCFtools (0.1.16)(55). Lastly, we estimated the ancestry for Green Bay, Muskegon Lake, and the five main basin sample sites, separately and jointly, with 10,000 randomly selected SNPs using Admixture 1.3(56) by setting *K* from 1 to 10.

Minor allele frequency, Tajima's D, and genetic diversity

Using the within-group data set, we calculated minor allele frequencies for seven sample sites and viewed its distribution by plotting density curves with unit bins of 0.015 with ggplot2(57) and ggridges in R 4.2.1(53). We calculated Tajima's D by setting the bin size to 5 MB with the within-group data set filtered by MAF $\geq$ 0.02 (Supplementary Table 3) using VCFtools (0.1.16). We estimated genetic diversity by calculating observed heterozygosity for every SNP and averaged observed heterozygosity across overlapping windows of 5 MB using a step size of 2.5 MB across each chromosome.

Effective population size and demographic history

We calculated effective population size with 30,000 randomly selected SNPs (replicated 3 times per population) for each population using the linkage disequilibrium method, as implemented in NeEstimator V2(23), by selecting the random mating model, setting the critical value to 0.05, and allowing for LD locus pairing across chromosomes. To further validate the *Ne* estimates, we calculated effective population size with 3,000 randomly selected SNPs from a previously

obtained RAD-Seq data set(58), again replicated 3 times per sample site for each of 12 sample sites (five from Green Bay, two from Grand Haven, two from Michigan City, one from Milwaukee, one from Naubinway, one from Sutton's Bay), using the same options described above. Returning to our whole-genome data sets, we reconstructed demographic histories by running GONE(34) with the within-group data set 100 times for each sample site. Meanwhile, we reconstructed the demographic history for Green Bay and Muskegon Lake by randomly selecting 30,000 SNPs from the within-group data set for each sample site (replicated 1000 times per sample site; Supplementary Table 3), converting VCF files into ped and map files in PLINK format using PLINK 2.0(59,60), and running GONE(34) for each of 1,000 randomly selected sets of 30,000 SNPs for each sample site using the default parameters. To verify demographic history reconstructed by GONE(34), we also ran Stairway Plot 2(33) for each of the seven sample sites with all biallelic SNPs that are genotyped for all samples in the corresponding sample site.

Candidate genes and gene ontology (GO) hierarchy networks underlying rapid adaptation

To calculate pairwise F_{ST} for pairs of populations (*i.e.*, Green Bay or Muskegon Lake *vs.* five main basin populations), we created a VCF file containing samples and their genotypic information in the two corresponding populations and filtered the VCF file following the same filtering processes for the within-group data set with MAF ≥ 0.05 across all samples in the two populations in comparison (see details in "Variant calling and filtering" in Supplementary Materials). To identify regions of the genome with overlapping windows of high F_{ST}, we first calculated pairwise Weir and Cockerham's F_{ST} with separate VCF files of pairs of populations using VCFtools (0.1.16)(55). We created ten separate F_{ST} files: five for each comparison between Green Bay and each of the five main basin sample sites (*i.e.*, Grand Haven, Michigan

City, Milwaukee, Naubinway, Sutton's Bay) and five for each comparison between Muskegon Lake and each of the five main basin sample sites. In all F_{ST} output files separately, we first identified SNPs that had $F_{ST} \geq 0.6$. We next took 10 KB steps in either direction of that SNP to identify all SNPs in that region. If additional SNPs in that region continued to have $F_{ST} \geq 0.6$, we continued to expand the window until no additional SNPs of high F_{ST} were found. For each comparison separately, we required that every window had a minimum of 50 SNPs, at least one of which had to have F_{ST} of 0.6 or higher. This step was implemented to filter out regions of the genome with very few segregating sites, which can indicate alignment or genome-assembly errors. We compared all windows to find windows that overlapped among the ten pairwise comparisons. To retain an outlier window, we required that a minimum of eight out of the ten windows shared at least one high F_{ST} SNP (note that despite this minimum requirement, all windows had at least 82 high F_{ST} SNPs). We mapped SNPs on outlier windows to the yellow perch genome(61) to identify candidate outlier genes potentially explaining parallel genetic adaptation in Green Bay and Muskegon Lake in comparison to main basin populations. We annotated candidate outlier genes using UniProtKB ID via UniProt (https://www.uniprot.org/), with which we retrieved gene ontology (GO) terms for these outlier genes from Gene Ontology and GO Annotations (https://www.ebi.ac.uk/QuickGO/). Lastly, we constructed GO hierarchy networks of GO terms associated with at least two outlier genes in the domain of "biological process" for each pairwise comparison (*i.e.*, Green Bay or Muskegon Lake *vs.* main basin populations) using the *metacoder*(62).

Water clarity, water quality, and phenotypic measurements

Water clarity was estimated using Secchi depth readings collected between June 1 and August 30 from Green Bay (320 readings), Muskegon Lake (72 readings), and the southern basin of Lake

Michigan (180 measurements) between 2010 and 2022. Data from Green Bay was provided for four offshore reference sites by the NEW Water monitoring project (www.newwater.us). Data for Muskegon Lake and Lake Michigan were collated from past and ongoing projects in the Höök Laboratory(63). Sample sites in Lake Michigan were located near large river mouths, but Secchi readings were taken outside of the river mouth plume. Therefore, these values represent conservatively low estimates of water clarity compared to offshore regions of Lake Michigan. In all cases, Secchi depth was collected using best practices of dropping a black and white Secchi disk on the shaded side of the boat and recording the depth in meters that it is no longer visible. We conducted an Analysis of Variance (ANOVA) test to determine whether there was a difference in Secchi depths among Green Bay, Muskegon Lake and the southern basin of Lake Michigan. Data on total phosphorus were taken from Fig. 2 (*i.e.*, average TP) in Harris et al.(64) for Green Bay and were extracted from Fig. 5c in Liu et al.(65) using WebPlotDigitizer (https://automeris.io/WebPlotDigitizer)(66) for Muskegon Lake.

We only collected fin clips from the 210 fish we sequenced, thus the fish measured for eye size were not the same set of fish that were genotyped. To collect yellow perch from the littoral zone of Muskegon Lake, boat electrofishing occurred at randomly selected sites around the perimeter of the lake in August 2022. Each site was electrofished for 20 minutes or until a total of 40 yellow perch of at least 150 mm in total length were collected. To collect yellow perch from Lake Michigan, the Michigan Department of Natural Resources set 4×2000 m experimental stretch mesh gill nets (3.81-15.24 cm) in 9-50 m of water overnight for 12.5-15 hours near the port of Grand Haven during May 2023. To collect yellow perch from Green Bay, the Michigan Department of Natural Resources set 4×97.5 m experimental stretch mesh gill nets (2.54-12.7 cm) in 6.4-9.5 m of water overnight for approximately 24 hours near the Menominee

River during September 2023. Yellow perch from both locations were transported to the laboratory where total body length was measured. Fish were individually marked (with a paper tag), fixed in 10% formalin for 6 days, and then transferred to 70% ethanol for long-term preservation. After 60 days in ethanol, eye diameters were measured using electronic calipers. To determine whether eye diameter differed among Green Bay, Muskegon Lake, and Lake Michigan, we analyzed yellow perch with total lengths of 150-250 mm to ensure comparisons of yellow perch with similar sizes among the three locations (*n=31* for Menominee in Green Bay, *n=39* for Muskegon Lake, and *n=27* for Grand Haven in Lake Michigan). With this subset of fish, we used Analysis of Covariance (ANCOVA) to test whether eye diameter differed among the three locations while accounting for total length as a covariate (including interaction between location and covariate). We compared least-squares means with Tukey's method using the "emmeans" function in the *emmeans* package in R (version 1.8.9).

Results

Population structure

We conducted whole-genome sequencing of 210 yellow perch samples from seven sample sites in Lake Michigan (Fig. 1a, Supplementary Table 1) resulting in an average sequencing depth of 12.50× across the genome. We mapped an average of 99.6% of 15.8 billion, 150 bp paired-end reads to the yellow perch genome(61) and, on average, over 90% and 83% of reads had a mapping quality equal to or greater than 20 or 60, respectively (Supplementary Table 2). We created two data sets based on different filtering criteria (see Methods): one data set where SNPs were excluded if the minor allele frequency (MAF) was smaller than 0.05 across all seven sample sites jointly (hereafter: **study-wide data set**) and a second data set where SNPs were excluded if the MAF was smaller than 0.05 within each population (hereafter: **within-group**

data set). The former was used for population genetic and stock identification analyses and the latter was used for demographic analyses (Supplementary Table 3). The study-wide data set resulted in 714,666 SNPs per sample site while the within-group data set resulted in an average of 1,160,504 SNPs with less than 0.9% of SNPs out of Hardy-Weinberg equilibrium in each sample site (Supplementary Table 4). After inferring phylogenetic relationships among populations, we found that Green Bay, Muskegon Lake, and the main basin sample sites (*i.e.*, Grand Haven, Michigan City, Milwaukee, Naubinway, and Sutton's Bay) form three distinct lineages (Fig. 1b, Supplementary Fig. 1). By conducting principal coordinate analysis with all individuals, we found further support that Green Bay, Muskegon Lake, and the main basin sample sites are clearly separated from each other (Fig. 1c, Supplementary Fig. 2a,b,c), except for one Muskegon Lake sample clustering with main basin populations and one Milwaukee main basin sample falling comparatively further away from the main basin populations (Fig. 1c, Supplementary Fig. 2d,e,f; see "Genetic divergence among yellow perch sample sites" and "Life history of yellow perch" in Supplementary Materials for details). This clear delineation of three populations was further supported by principal coordinate analysis on the mean pairwise estimates of F_{ST} where we detected high genetic differentiation between Green Bay and Muskegon Lake (F_{ST} = 0.0520), both of which are genetically divergent from the five main basin sample sites (F_{ST} = 0.0550 to 0.0667, 0.0460 to 0.0592, respectively; Supplementary Table 5, Supplementary Fig. 3a). By contrast, the five main basin sample sites are comparatively similar to each other, with mean pairwise F_{ST} ranging from -0.0002 to 0.0041 (Supplementary Table 5, Supplementary Fig. 3b). The optimal number of clusters/populations identified with admixture analysis(56) for all populations was 3: Green Bay, Muskegon Lake, and the main basin sample sites (Fig. 1d, Supplementary Fig. 4).

Numbers of SNPs, minor allele frequency, and Tajima's D

When using the within-group data set, we detected 2.8-3.4 times more polymorphic SNPs in Green Bay and Muskegon Lake sample sites, respectively, in comparison to the main basin sample sites (2,186,768 and 2,275,935 *vs.* 670,578 to 776,088 SNPs in main basin populations; Fig. 2a). The median minor allele frequency of SNPs was 0.086 and 0.083 in Green Bay and Muskegon Lake, respectively, which was 0.46 times lower than that in main basin populations, which ranged from 0.183 to 0.185 (Fig. 2b). These differences in the number of SNPs and median minor allele frequencies were not driven by differences in sample sizes (Supplementary Table 1), sequencing quality (see "Whole-genome sequencing" in Supplementary Materials for details), sequencing depth (Supplementary Table 6), read depth of aligned reads (Supplementary Table 7), or missing data (see "Variant calling and filtering" in Supplementary Materials for details). Using the within-group data set, we observed consistently positive Tajima's D values in the main basin populations, varying from 0.332 to 0.428 on average, which is suggestive of slight population declines in the main basin (Fig. 2c). By contrast, Green Bay and Muskegon Lake populations had a genome-wide average Tajima's D of -0.632 and -0.603, respectively (Fig. 2c), which is suggestive of a recent demographic expansion.

Effective population size, genetic diversity, and demographic history

In comparison to the main basin sample sites, Green Bay and Muskegon Lake have significantly lower effective population sizes, the point estimates of which were 23 and 90, respectively (Fig. 3a). Effective population size estimates using a RAD-Seq data set with larger numbers of samples(58), but smaller numbers of loci, suggest that southern and middle Green Bay (SGB, MEN) have smaller effective population sizes than northern Green Bay (BDN, LBD), with high levels of concurrence between both data sets, suggesting that main basin sample sites have

considerably larger effective population sizes (Fig. 3b). Genetic diversity of main basin sample sites, with a mean observed heterozygosity ranging from 0.312 to 0.323, was considerably higher than that of Green Bay and Muskegon Lake populations, with a mean observed heterozygosity of 0.208 and 0.206, respectively (Fig. 3c, Supplementary Fig. 5). Despite Green Bay and Muskegon Lake having a greater number of SNPs, the lower observed heterozygosity is predicted from theory given the much lower average allele frequencies. GONE, based on patterns of linkage disequilibrium (LD), can reconstruct reliable demographic histories for recent generations despite potential noises from genotyping errors, nonrandom mating, population admixture, overlapping generations, and genetic map alterations(34). Using this approach, we reconstructed contemporary demographic histories and found that Green Bay and Muskegon Lake experienced rapid growth of *Ne* in their most recent generations (Fig. 3d,e, Supplementary Fig. 6). Stairway Plot 2(33), based on site frequency spectra, suggests increases in *Ne* in Green Bay and Muskegon Lake since around 1000 years ago and in main basin populations since around 2000 to 3000 years ago (Supplementary Fig. 7).

Candidate genes underlying genetic adaptation

Given the high levels of genetic divergence between Green Bay, Muskegon, and the main basin sites, we used a genome-wide scan to determine if any regions of the genome are suggestive of genetic adaptation to the different environments(67,68). We retained a total of 13 outlier windows from nine chromosomes that were shared in at least 80% of comparisons between Green Bay and the main basin collection sites as well as Muskegon Lake and the main basin populations (see Methods; Supplementary Table 8). The 13 outlier windows contained an average of 1,427 SNPS (range: 363-3,203) and an average of 225 high F_{ST} SNPs ($F_{ST} \geq 0.6$; range 82-360 SNPs per window) (Fig. 4a). SNPs within these 13 outlier windows map to 36

genes, among which three were located within a single outlier window on chromosome 4 (chromosome 4: 34762415-34852528). The three genes, *opn1sw*, *opn1lw*, and *opn1lw2*, encode visual pigments, light-absorbing molecules mediating vision. Out of the three visual pigment-encoding genes, *opn1lw2* has two outlier SNPs with $F_{ST} \geq 0.5$ in comparisons between Green Bay and the main basin sample sites, and the exact same two outlier SNPs, one with $F_{ST} \geq 0.76$ and the other with $F_{ST} \geq 0.46$, were found in comparisons between Muskegon Lake and the main basin sample sites (Fig. 4a). The observation that three visual pigment-encoding genes were found on the same outlier window in all ten pairwise comparisons suggests that this region has responded to recent positive and parallel selection. Across all outlier windows, seven major categories of biological processes were detected between Green Bay and the main basin sample sites and Muskegon Lake and the main basin sample sites: multicellular organismal process, response to stimulus, biological regulation, cellular process, developmental process, localization, and metabolic process (Fig. 4b). Multiple visual perception-related biological processes, including detection of visible light, absorption of visible light, visual perception, cellular response to light stimulus, and phototransduction, provide further support for parallel adaptive differences in vision in Green Bay and Muskegon Lake yellow perch populations (Fig. 4b). Using these genomic data to develop *a priori* hypotheses for subsequent environmental and phenotypic data, we hypothesized that water clarity and eye size would differ between the two sites (Green Bay and Muskegon Lake) and the main basin. We found significant differences in water clarity between the main basin of Lake Michigan (low turbidity, high visual clarity; mean Secchi depth ± s.d.: 6.10 ± 3.23 m) and both Green Bay (high turbidity, low visual clarity; 1.59 ± 1.01 m) and Muskegon Lake (high turbidity, low visual clarity; 2.48 ± 1.23 m; ANOVA, $P < 0.001$; Fig. 4c). We also found that yellow perch eye diameter differed among locations

(ANCOVA, $F_{2,91}$ = 12.03; P < 0.001) and significantly increased with total length (ANCOVA, $F_{1,91}$ = 45.67; P < 0.001), but the interaction was not significant (ANCOVA, $F_{2,91}$ = 0.11; P = 0.779; Supplementary Fig. 8). Yellow perch eye diameter was significantly larger for Muskegon Lake than the main basin (Grand Haven; P < 0.001) and Green Bay (near Menominee; P < 0.001), and Green Bay was also significantly larger than the main basin (P < 0.001; Fig. 4d).

Discussion

Using whole-genome sequence data from 210 yellow perch, we observed multiple genomic signatures associated with demographic increases in Green Bay and Muskegon Lake where: (1) effective population sizes rapidly increased for the last several generations, (2) Tajima's D estimates were negative across the entire genome, and (3) a factor of 2.8-3.4 more polymorphic SNPs were found in Green Bay and Muskegon Lake than the main basin collection sites, where the majority of these additional SNPs occur at low frequency. This last observation is consistent with a large, recent (over evolutionary time) population expansion where there has not been sufficient time for negative selection to remove deleterious alleles(69).

To what time period do our demographic inferences apply? Linkage disequilibrium based methods of *Ne*, such as those depicted in Fig. 3, provide recent and contemporary estimates of effective population size (70). We used the program GONE to estimate recent changes to *Ne* over time and the results suggest that there have been contemporary increases in *Ne* in both Green Bay and Muskegon Lake. However, the exact date for when these increases in *Ne* began remains imprecise. A recent study with pink salmon (*Oncorhynchus gorbuscha*) and a known date of an extreme founder event illustrated that GONE may have missed the timing of the event by as much as 6 generations (39). Nevertheless, the known abundance patterns in salmon and other species are well characterized with this approach(39,71) and our results clearly illustrate

that effective population sizes have been increasing in both Muskegon and Green Bay in the last 10 to 50 generations, with larger increases occurring in Muskegon Lake. Our inferences based on Tajima's D, the number of segregating loci, and site frequency spectra suggest much larger increases in *Ne* that occurred over much longer timescales (centuries, not decades) (Fig. 2; Supplementary Fig. 7). This result contrasts with those from main basin sites, which all show increases in *Ne* starting more than 2000 years ago and no signs of a historic bottleneck (Supplementary Fig. 7). We speculate that both the Green Bay and the Muskegon Lake yellow perch populations were founded much more recently than the main basin populations or that both went through a large, unknown, bottleneck event approximately 1,000 years ago.

The results from this study are striking for several reasons. First, for there to be genome-wide signals of population expansion means that the effect size is likely to be very large. Stated differently, the fact that we can detect genomic signals of population expansion suggest that adult abundances have increased rapidly and likely by several orders of magnitude(6,9–11,72). Second, it is of note that the increases in contemporary (LD) estimates of effective population size coincide with the wide-scale clean-up efforts in both Green Bay and Muskegon Lake and corresponding reductions in excess nutrients and other pollutants (see Supplementary Discussion). Third, in comparison to the main basin of Lake Michigan, both Green Bay and Muskegon Lake exhibit high turbidity and low visual clarity, as indicated by shallower Secchi depths. Such differences in water clarity and ambient light conditions could have driven the significant allele frequency shifts in the coding sequences of photopigment encoding genes and triggered a set of biological processes contributing to light detection and absorption, visual perception, and phototransduction, a result that implies parallel genetic adaptation in Green Bay and Muskegon Lake yellow perch in response to local environmental conditions.

Several caveats are worth discussing. First, linkage disequilibrium based estimates of effective population sizes may not accurately estimate effective population sizes prior to bottleneck events(39,73). As such, the effective population sizes of yellow perch in Green Bay and Muskegon Lake prior to around 30 generations ago were likely much larger than present day estimates but cannot be estimated using those approaches. Demographic estimates using site frequency spectra analyses suggest that effective population sizes may have been in the hundreds of thousands of individuals in both Green Bay and Muskegon Lake prior to increased anthropogenic disturbances (Supplementary Fig. 7). Second, some of our demographic results could also be explained by introgression from neighboring populations, however, we do not think this to be the case because: 1.) The primary yellow perch population connected to Muskegon Lake (the site with the largest increase in *Ne*) is the main basin population. Even if all of the main basin loci were introduced into Muskegon Lake samples via introgression (which is unlikely), this mechanism could only account for 24% of the 2,275,935 SNPs found in Muskegon Lake (*i.e.*, 535,860 SNPs shared by Muskegon Lake and Grand Haven divided by 2,275,935 Muskegon Lake SNPs; Fig. 2A), 2.) over shorter time scales, estimates of contemporary admixture within Green Bay and Muskegon Lake samples suggest a single, randomly mating population (as do the small number of loci out of Hardy-Weinberg equilibrium (HWE)) (Supplementary Fig. 4; Table S4), and 3.) over longer time scales, the high rates of introgression required to explain these results would also be likely to swamp any signal of parallel genetic adaptation (Fig. 4) and would also leave more time for purifying selection to remove deleterious loci. Note that other factors that can increase *Ne* through time (*e.g.*, decreased variance in reproductive success) are highly unlikely to be accompanied by the other genomic patterns we report (*i.e.*, negative Tajima's D, larger numbers of SNPs). Thus, we think the most

parsimonious explanation for our results may be large, simultaneous increases in population sizes in Green Bay and Muskegon Lake yellow perch. By contrast, fisheries independent data suggest that yellow perch have been recently declining in the main basin(74) and the positive, albeit small, genome-wide estimates of Tajima's D suggest that these populations should be closely monitored in the coming decades.

In conclusion, we found that two populations of an economically important fish species have had large, simultaneous increases in effective population sizes both historically and over contemporary timescales. The two populations are separated by over 350 km and are genetically divergent from one another, such that they essentially represent two distinct lineages (Fig. 1b). We also found evidence of parallel adaptation to reduced visual clarity in each of the habitats, which may also have been driven by centuries-long anthropogenic disturbances and pollution, though we suspect that this genetic adaptation occurred over a longer timescale than the recent demographic recoveries. The contemporary estimates of *Ne* are orders of magnitude lower than historic estimates, suggesting that recent anthropogenic disturbances may have reduced genetic diversity in Green Bay and Muskegon Lake. Nevertheless, the recent increases in *Ne* suggest that the largest threats to these populations may have passed. Taken together, these results suggest that the synchrony of key ecological and evolutionary processes can drive parallel demographic and evolutionary trajectories across independent populations. How frequently such synchrony occurs remains an open question in the fields of ecology and evolution.

Data availability

All raw data generated for this project are stored in the NCBI Short Read Archive (SRA). Additionally, unfiltered and filtered VCF files (as described in Supplementary Table 3) are also

available at figshare. The scripts used in this project are hosted in a public repository and archived at PURR (Repo).

References

1. Wright S. Evolution in Mendelian Populations. Genetics. 1931 Mar;16(2):97–159.

2. Hedgecock D, Pudovkin A. Sweepstakes Reproductive Success in Highly Fecund Marine Fish and Shellfish: A Review and Commentary. Bulletin of Marine Science. 2011 Oct 1;87:971–1002.

3. Hedgecock D. Does variance in reproductive success limit effective population sizes of marine organisms? Genetics and Evolution of Aquatic Organisms. 1994 Jan 1;

4. Hahn M. Molecular Population Genetics. Oxford, New York: Oxford University Press; 2018. 352 p.

5. Frankham R. Effective population size/adult population size ratios in wildlife: A review. Genetical Research [Internet]. 1995 [cited 2024 Feb 21];66(2):95–107. Available from: http://www.scopus.com/inward/record.url?scp=0028874989&partnerID=8YFLogxK

6. Hauser L, Adcock GJ, Smith PJ, Ramiréz JHB, Carvalho GR. Loss of microsatellite diversity and low effective population size in an overexploited population of New Zealand snapper (*Pagrus auratus*). Proceedings of the National Academy of Sciences of the United States of America. 2002 Sep 3;99(18):11742–7.

7. Hoarau G, Boon E, Jongma DN, Ferber S, Palsson J, Van der Veer HW, et al. Low effective population size and evidence for inbreeding in an overexploited flatfish, plaice (*Pleuronectes platessa* L.). Proc Biol Sci. 2005 Mar 7;272(1562):497–503.

8. Laurent V, Planes S. Effective population size estimation on *Sardina pilchardus* in the Bay of Biscay using a temporal genetic approach. Biological Journal of the Linnean Society [Internet]. 2007 Apr 1 [cited 2024 Feb 21];90(4):591–602. Available from: https://doi.org/10.1111/j.1095-8312.2007.00747.x

9. Abadía-Cardoso A, Freimer NB, Deiner K, Garza JC. Molecular population genetics of the northern elephant seal *Mirounga angustirostris*. J Hered [Internet]. 2017 Sep [cited 2023 Sep 30];108(6):618–27. Available from: https://www.ncbi.nlm.nih.gov/pmc/articles/PMC5892393/

10. Miller LM, Kapuscinski AR. Historical analysis of genetic variation reveals low effective population size in a northern pike (*Esox Lucius*) population. Genetics [Internet]. 1997 Nov [cited 2023 Oct 20];147(3):1249–58. Available from: https://www.ncbi.nlm.nih.gov/pmc/articles/PMC1208248/

11. Turner TF, Wares JP, Gold JR. Genetic effective size is three orders of magnitude smaller than adult census size in an abundant, Estuarine-dependent marine fish (*Sciaenops ocellatus*). Genetics. 2002 Nov;162(3):1329–39.

12. Hutchinson WF, van Oosterhout C, Rogers SI, Carvalho GR. Temporal analysis of archived samples indicates marked genetic changes in declining North Sea cod (*Gadus morhua*). Proc Biol Sci [Internet]. 2003 Oct 22 [cited 2024 Feb 12];270(1529):2125–32. Available from: https://www.ncbi.nlm.nih.gov/pmc/articles/PMC1691486/

13. Capblancq T, Butnor JR, Deyoung S, Thibault E, Munson H, Nelson DM, et al. Whole-exome sequencing reveals a long-term decline in effective population size of red spruce (*Picea rubens*). Evol Appl [Internet]. 2020 May 22 [cited 2024 Feb 11];13(9):2190–205. Available from: https://www.ncbi.nlm.nih.gov/pmc/articles/PMC7513712/

14. Sharma R, Arora N, Goossens B, Nater A, Morf N, Salmona J, et al. Effective population size dynamics and the demographic collapse of Bornean orang-utans. PLOS ONE [Internet]. 2012 Nov 15 [cited 2024 Feb 11];7(11):e49429. Available from: https://journals.plos.org/plosone/article?id=10.1371/journal.pone.0049429

15. Okello JBA, Wittemyer G, Rasmussen HB, Arctander P, Nyakaana S, Douglas-Hamilton I, et al. Effective population size dynamics reveal impacts of historic climatic events and recent anthropogenic pressure in African elephants. Mol Ecol. 2008 Sep;17(17):3788–99.

16. Ólafsdóttir GÁ, Westfall KM, Edvardsson R, Pálsson S. Historical DNA reveals the demographic history of Atlantic cod (*Gadus morhua*) in medieval and early modern Iceland. Proceedings of the Royal Society B: Biological Sciences [Internet]. 2014 Feb 22 [cited 2024 Feb 11];281(1777):20132976. Available from: https://royalsocietypublishing.org/doi/10.1098/rspb.2013.2976

17. Lonsinger RC, Adams JR, Waits LP. Evaluating effective population size and genetic diversity of a declining kit fox population using contemporary and historical specimens. Ecol Evol [Internet]. 2018 Nov 8 [cited 2024 Feb 11];8(23):12011–21. Available from: https://www.ncbi.nlm.nih.gov/pmc/articles/PMC6303725/

18. Pita A, Pérez M, Velasco F, Presa P. Trends of the genetic effective population size in the Southern stock of the European hake. Fisheries Research [Internet]. 2017 Jul 1 [cited 2024 Feb 12];191:108–19. Available from: https://www.sciencedirect.com/science/article/pii/S0165783617300590

19. Ovenden JR, Leigh GM, Blower DC, Jones AT, Moore A, Bustamante C, et al. Can estimates of genetic effective population size contribute to fisheries stock assessments? Journal of Fish Biology [Internet]. 2016 [cited 2024 Feb 11];89(6):2505–18. Available from: https://onlinelibrary.wiley.com/doi/abs/10.1111/jfb.13129

20. Hare MP, Nunney L, Schwartz MK, Ruzzante DE, Burford M, Waples RS, et al. Understanding and estimating effective population size for practical application in marine species management. Conserv Biol. 2011 Jun;25(3):438–49.

21. Shrimpton JM, Heath DD. Census vs. effective population size in chinook salmon: large- and small-scale environmental perturbation effects. Mol Ecol. 2003 Oct;12(10):2571–83.

22. Horreo J, Machado-Schiaffino G, Griffiths A, Bright D, Stevens J, Garcia-Vazquez E. Atlantic salmon at risk: Apparent rapid declines in effective population size in southern European populations. Transactions of the American Fisheries Society. 2011 May 1;140:605–10.

23. Do C, Waples RS, Peel D, Macbeth GM, Tillett BJ, Ovenden JR. NeEstimator v2: re-implementation of software for the estimation of contemporary effective population size (*Ne*) from genetic data. Molecular Ecology Resources [Internet]. 2014 [cited 2022 Jul 14];14(1):209–14. Available from: https://onlinelibrary.wiley.com/doi/abs/10.1111/1755-0998.12157

24. Nomura T. Estimation of effective number of breeders from molecular coancestry of single cohort sample. Evol Appl [Internet]. 2008 Aug [cited 2024 Feb 14];1(3):462–74. Available from: https://www.ncbi.nlm.nih.gov/pmc/articles/PMC3352377/

25. Cowen R, Gawarkiewicz G, Pineda J, Thorrold S, Werner F. Population connectivity in marine systems: An overview. Oceanography. 2007 Sep 1;20.

26. Cowen RK, Sponaugle S. Larval dispersal and marine population connectivity. Annual Review of Marine Science [Internet]. 2009 [cited 2024 Feb 21];1(1):443–66. Available from: https://doi.org/10.1146/annurev.marine.010908.163757

27. Waples R. Separating the wheat from the chaff: patterns of genetic differentiation in high gene flow species. Journal of Heredity [Internet]. 1998 Sep 1 [cited 2024 Feb 21];89(5):438–50. Available from: https://doi.org/10.1093/jhered/89.5.438

28. Christie MR, Tissot BN, Albins MA, Beets JP, Jia Y, Ortiz DM, et al. Larval connectivity in an effective network of marine protected areas. PLOS ONE [Internet]. 2010 Dec 21 [cited 2022 Sep 15];5(12):e15715. Available from: https://journals.plos.org/plosone/article?id=10.1371/journal.pone.0015715

29. Waples RS. Practical application of the linkage disequilibrium method for estimating contemporary effective population size: A review. Molecular Ecology Resources [Internet]. 2024 [cited 2024 Feb 21];24(1):e13879. Available from: https://onlinelibrary.wiley.com/doi/abs/10.1111/1755-0998.13879

30. Palstra FP, Ruzzante DE. Genetic estimates of contemporary effective population size: What can they tell us about the importance of genetic stochasticity for wild population persistence? Mol Ecol. 2008 Aug;17(15):3428–47.

31. Jorde PE, Ryman N. Temporal allele frequency change and estimation of effective size in populations with overlapping generations. Genetics. 1995 Feb;139(2):1077–90.

32. Liu X, Fu YX. Exploring population size changes using SNP frequency spectra. Nat Genet [Internet]. 2015 May [cited 2024 Feb 14];47(5):555–9. Available from: https://www.nature.com/articles/ng.3254

33. Liu X, Fu YX. Stairway Plot 2: demographic history inference with folded SNP frequency spectra. Genome Biology [Internet]. 2020 Nov 17 [cited 2022 Jul 14];21(1):280. Available from: https://doi.org/10.1186/s13059-020-02196-9

34. Santiago E, Novo I, Pardiñas AF, Saura M, Wang J, Caballero A. Recent demographic history inferred by high-resolution analysis of linkage disequilibrium. Molecular Biology and Evolution [Internet]. 2020 Dec 16 [cited 2022 Sep 17];37(12):3642–53. Available from: https://doi.org/10.1093/molbev/msaa169

35. Gutenkunst RN, Hernandez RD, Williamson SH, Bustamante CD. Inferring the joint demographic history of multiple populations from multidimensional SNP frequency data. PLoS Genet. 2009 Oct;5(10):e1000695.

36. Li H, Durbin R. Inference of human population history from individual whole-genome sequences. Nature [Internet]. 2011 Jul [cited 2024 Feb 23];475(7357):493–6. Available from: https://www.nature.com/articles/nature10231

37. Westbury MV, Hartmann S, Barlow A, Wiesel I, Leo V, Welch R, et al. Extended and continuous decline in effective population size results in low genomic diversity in the world's rarest hyena species, the brown hyena. Shapiro B, editor. Molecular Biology and Evolution [Internet]. 2018 May 1 [cited 2024 Feb 11];35(5):1225–37. Available from: https://academic.oup.com/mbe/article/35/5/1225/4924857

38. Diaz M, Wethey D, Bulak J, Ely B. Effect of harvest and effective population size on genetic diversity in a striped bass population. Transactions of the American Fisheries Society [Internet]. 2000 Nov 1;129(6):1367–72. Available from: https://scholarcommons.sc.edu/biol_facpub/48

39. Sparks MM, Schraidt CE, Yin X, Seeb LW, Christie MR. Rapid genetic adaptation to a novel ecosystem despite a large founder event. Mol Ecol. 2023 Sep 5;

40. Hoey JA, Able KW, Pinsky ML. Genetic decline and recovery of a demographically rebuilt fishery species. Molecular Ecology [Internet]. 2022 [cited 2024 Feb 12];31(22):5684–98. Available from: https://onlinelibrary.wiley.com/doi/abs/10.1111/mec.16697

41. Wang J, Santiago E, Caballero A. Prediction and estimation of effective population size. Heredity [Internet]. 2016 Oct [cited 2024 Feb 12];117(4):193–206. Available from: https://www.nature.com/articles/hdy201643

42. Hedrick P. Large variance in reproductive success and the Ne/N ratio. Evolution [Internet]. 2005 [cited 2024 Feb 12];59(7):1596–9. Available from: https://www.jstor.org/stable/3449182

43. Allendorf FW. Delay of adaptation to captive breeding by equalizing family size. Conservation Biology [Internet]. 1993 [cited 2024 Feb 12];7(2):416–9. Available from: https://www.jstor.org/stable/2386440

44. Borlase S, Loebel D, Frankham R, Nurthen R, Briscoe D, Daggard GE. Modeling problems in conservation genetics using captive *Drosophila* populations: consequences of equalization of family sizes. Conservation Biology. 2002 Feb 23;7:122–31.

45. Waples RS, Hindar K, Karlsson S, Hard JJ. Evaluating the Ryman–Laikre effect for marine stock enhancement and aquaculture. Curr Zool [Internet]. 2016 Dec [cited 2024 Feb 23];62(6):617–27. Available from: https://www.ncbi.nlm.nih.gov/pmc/articles/PMC5804264/

46. Ryman N, Laikre L. Effects of supportive breeding on the genetically effective population size. Conservation Biology [Internet]. 1991 [cited 2024 Feb 23];5(3):325–9. Available from: https://onlinelibrary.wiley.com/doi/abs/10.1111/j.1523-1739.1991.tb00144.x

47. Baldwin N, Saalfeld R, Dochoda M, Buettner H, Eshenroder R. Commercial fish production in the Great Lakes 1867-2006 [online]. Available from http://www.glfc.org/databases/commercial/commerc.php. 2009;

48. Kinnunen R. Great Lakes commercial fisheries. Michigan Sea Grant. 2003;

49. Marsden JE, Robillard SR. Decline of yellow perch in southwestern Lake Michigan, 1987–1997. North American Journal of Fisheries Management [Internet]. 2004 [cited 2023 Oct 20];24(3):952–66. Available from: https://onlinelibrary.wiley.com/doi/abs/10.1577/M02-195.1

50. McKenna A, Hanna M, Banks E, Sivachenko A, Cibulskis K, Kernytsky A, et al. The Genome Analysis Toolkit: A MapReduce framework for analyzing next-generation DNA sequencing data. Genome Res [Internet]. 2010 Sep 1 [cited 2020 Jan 17];20(9):1297–303. Available from: http://genome.cshlp.org/content/20/9/1297

51. Stamatakis A. RAxML version 8: a tool for phylogenetic analysis and post-analysis of large phylogenies. Bioinformatics. 2014 May 1;30(9):1312–3.

52. Tamura K, Stecher G, Kumar S. MEGA11: Molecular evolutionary genetics analysis version 11. Molecular Biology and Evolution [Internet]. 2021 Jul 1 [cited 2022 Jul 19];38(7):3022–7. Available from: https://doi.org/10.1093/molbev/msab120

53. R Core Team. R: A language and environment for statistical computing. R Foundation for Statistical Computing, Vienna, Austria. URL https://www.R-project.org/. 2020;

54. Peakall R, Smouse PE. GenAlEx 6.5: genetic analysis in Excel. Population genetic software for teaching and research—an update. Bioinformatics [Internet]. 2012 Oct 1 [cited 2022 Aug 12];28(19):2537–9. Available from: https://www.ncbi.nlm.nih.gov/pmc/articles/PMC3463245/

55. Weir BS, Cockerham CC. Estimating F-statistics for the analysis of population structure. Evolution [Internet]. 1984 [cited 2020 Jan 18];38(6):1358–70. Available from: https://www.jstor.org/stable/2408641

56. Alexander DH, Novembre J, Lange K. Fast model-based estimation of ancestry in unrelated individuals. Genome Res. 2009 Sep;19(9):1655–64.

57. Wickham H. ggplot2: Elegant Graphics for Data Analysis. 1st ed. 2009. Corr. 3rd printing 2010 edition. New York: Springer; 2010. 213 p.

58. Schraidt CE, Ackiss AS, Larson WA, Rowe MD, Höök TO, Christie MR. Dispersive currents explain patterns of population connectivity in an ecologically and economically important fish. Evolutionary Applications [Internet]. 2023 [cited 2023 Sep 10];16(7):1284–301. Available from: https://onlinelibrary.wiley.com/doi/abs/10.1111/eva.13567

59. Chang CC, Chow CC, Tellier LC, Vattikuti S, Purcell SM, Lee JJ. Second-generation PLINK: rising to the challenge of larger and richer datasets. GigaScience [Internet]. 2015 Dec 1 [cited 2022 Sep 17];4(1):s13742-015-0047–8. Available from: https://doi.org/10.1186/s13742-015-0047-8

60. Purcell S, Chang C. PLINK 2.0. Available from: www.cog-genomics.org/plink/2.0/

61. Feron R, Zahm M, Cabau C, Klopp C, Roques C, Bouchez O, et al. Characterization of a Y-specific duplication/insertion of the anti-Mullerian hormone type II receptor gene based on a chromosome-scale genome assembly of yellow perch, *Perca flavescens*. Molecular Ecology Resources [Internet]. 2020 [cited 2022 Jul 14];20(2):531–43. Available from: https://onlinelibrary.wiley.com/doi/abs/10.1111/1755-0998.13133

62. Foster ZSL, Sharpton TJ, Grünwald NJ. Metacoder: An R package for visualization and manipulation of community taxonomic diversity data. PLOS Computational Biology [Internet]. 2017 Feb 21 [cited 2020 Jan 18];13(2):e1005404. Available from: https://journals.plos.org/ploscompbiol/article?id=10.1371/journal.pcbi.1005404

63. Jameel Y, Stein S, Grimm E, Roswell C, Wilson AE, Troy C, et al. Physicochemical characteristics of a southern Lake Michigan river plume. Journal of Great Lakes Research [Internet]. 2018 Apr 1 [cited 2023 Oct 20];44(2):209–18. Available from: https://www.sciencedirect.com/science/article/pii/S0380133018300042

64. Harris HJ, Wenger RB, Sager PE, Val Klump J. The Green Bay saga: Environmental change, scientific investigation, and watershed management. Journal of Great Lakes Research [Internet]. 2018 Oct 1 [cited 2023 Sep 24];44(5):829–36. Available from: https://www.sciencedirect.com/science/article/pii/S0380133018301412

65. Liu B, McLean CE, Long DT, Steinman AD, Stevenson RJ. Eutrophication and recovery of a lake inferred from sedimentary diatoms originating from different habitats. Science of The Total Environment [Internet]. 2018 Jul 1 [cited 2023 Sep 24];628–629:1352–61. Available from: https://www.sciencedirect.com/science/article/pii/S0048969718305679

66. Rohatgi A. WebPlotDigitizer. 2022 Sep; Available from: https://automeris.io/WebPlotDigitizer

67. Willoughby JR, Harder AM, Tennessen JA, Scribner KT, Christie MR. Rapid genetic adaptation to a novel environment despite a genome-wide reduction in genetic diversity. Mol Ecol. 2018;27(20):4041–51.

68. Bernatchez L, Ferchaud AL, Berger CS, Venney CJ, Xuereb A. Genomics for monitoring and understanding species responses to global climate change. Nat Rev Genet [Internet]. 2024 Mar [cited 2024 Feb 23];25(3):165–83. Available from: https://www.nature.com/articles/s41576-023-00657-y

69. Marth GT, Czabarka E, Murvai J, Sherry ST. The allele frequency spectrum in genome-wide human variation data reveals signals of differential demographic history in three large world populations. Genetics. 2004 Jan;166(1):351–72.

70. Waples RS, Do C. Linkage disequilibrium estimates of contemporary Ne using highly variable genetic markers: a largely untapped resource for applied conservation and evolution. Evol Appl [Internet]. 2010 May [cited 2024 Mar 4];3(3):244–62. Available from: https://www.ncbi.nlm.nih.gov/pmc/articles/PMC3352464/

71. Kardos M, Zhang Y, Parsons KM, A Y, Kang H, Xu X, et al. Inbreeding depression explains killer whale population dynamics. Nat Ecol Evol [Internet]. 2023 May [cited 2024 Mar 4];7(5):675–86. Available from: https://www.nature.com/articles/s41559-023-01995-0

72. Gaut BS, Seymour DK, Liu Q, Zhou Y. Demography and its effects on genomic variation in crop domestication. Nature Plants [Internet]. 2018 Aug [cited 2023 Nov 4];4(8):512–20. Available from: https://www.nature.com/articles/s41477-018-0210-1

73. Reid BN, Pinsky ML. Simulation-based evaluation of methods, data types, and temporal sampling schemes for detecting recent population declines. Integr Comp Biol. 2022 Dec 30;62(6):1849–63.

74. Clapp D, Makauskas D. Status of yellow perch in Lake Michigan - 2019-2020. Report to the Lake Michigan committee. 2021;

Figure Legends

Fig. 1. Population structure of Lake Michigan yellow perch populations. Yellow perch collected from seven Lake Michigan sites (a), including the comparatively isolated Muskegon Lake, which is connected to the main basin by a narrow channel (see inset). A phylogenetic tree illustrates three distinct groups: Green Bay, Muskegon Lake, and the five main basin sample sites (b). Twenty-five main basin individuals were randomly sampled for visual clarity; see Supplementary Fig. 1 for the full phylogenetic tree with all 210 individuals. Both principal coordinate analysis of 210 individuals (c) and admixture analyses (d) further support the delineation of samples into three discrete populations. Notice that one individual sampled in Muskegon Lake likely swam in from the main basin (Supplementary Fig. 2; see "Genetic divergence among yellow perch sample sites" in Supplementary Materials for details).

Fig. 2. Numbers of single nucleotide polymorphisms (SNPs), minor allele frequency, and Tajima's D. Green Bay and Muskegon Lake populations have 2.8-3.4 times more SNPs than the five main basin sample sites (a), despite all sample sites having equal sample sizes, sequencing quality, read depth, and missing data. Both Green Bay and Muskegon Lake also have a lower median minor allele frequency compared to the five main basin populations (b) here illustrated with a density plot where the median minor allele frequency is depicted with a solid vertical line. The negative Tajima's D for both Green Bay and Muskegon Lake populations suggests recent population expansion (c). Collectively, these results suggest that the three populations (Green Bay, Muskegon Lake, and the main basin sample sites) have different demographic histories.

Fig. 3. Demographic history of Lake Michigan yellow perch populations. Green Bay and Muskegon Lake sample sites have substantially lower effective population sizes, which average 23 and 90, respectively, in comparison to main basin populations (a,b; note that y-axis is on a base 10 logarithmic scale; SGB: South Green Bay, MUS: Muskegon, GRH: Grand Haven, MIC: Michigan City, MIL: Milwaukee, NUB: Naubinway, SUT: Sutton's Bay, MEN: Menominee, BDN: Big Bay de Noc, LBD: Little Bay de Noc). Green Bay and Muskegon Lake have lower genetic diversity (c) than main basin populations, measured here as observed heterozygosity averaged across overlapping windows of 5 MB using a step size of 2.5 MB across each chromosome. Notice that the main basin heterozygosity estimates are highly correlated, confirming higher gene flow among main basin sample sites. The demographic history, as reconstructed by GONE, demonstrates a rapid increase in effective population size in Green Bay and Muskegon Lake in their most recent generations (d,e).

Fig. 4. Candidate genes, biological processes, and phenotypes involved in parallel genetic adaptation. A total of 13 outlier windows were detected in comparisons between both Green Bay and the main basin sample sites and Muskegon Lake and the main basin sample sites (a). The outlier window on chromosome 4 contains visual pigment encoding genes, such as *opn1lw2*. The coding regions, as indicated by horizontal gray bars, of these outlier genes contain SNPs that are highly differentiated (a). Seven major categories of biological processes are potentially involved in adaptive differentiation in Green Bay and Muskegon Lake in comparison to main basin sample sites, among which visual perception-related processes (highlighted with red asterisks) further support parallel adaptive differences in vision in Green Bay and Muskegon

Lake (b). The genetic differentiation at *opn1lw2* is likely associated with water clarity, as evidenced by significant differences in Secchi depths (c) and different eye sizes (d) between Green Bay or Muskegon Lake and main basin populations (*i.e.*, Lake Michigan, Grand Haven). The Secchi depth in Green Bay and Muskegon Lake is significantly smaller than that in the southern basin of Lake Michigan ($P < 0.001$; c) and least-squares means of yellow perch eye diameter in Green Bay and Muskegon Lake is significantly larger than that in Grand Haven ($P < 0.001$; d).

Figure 1

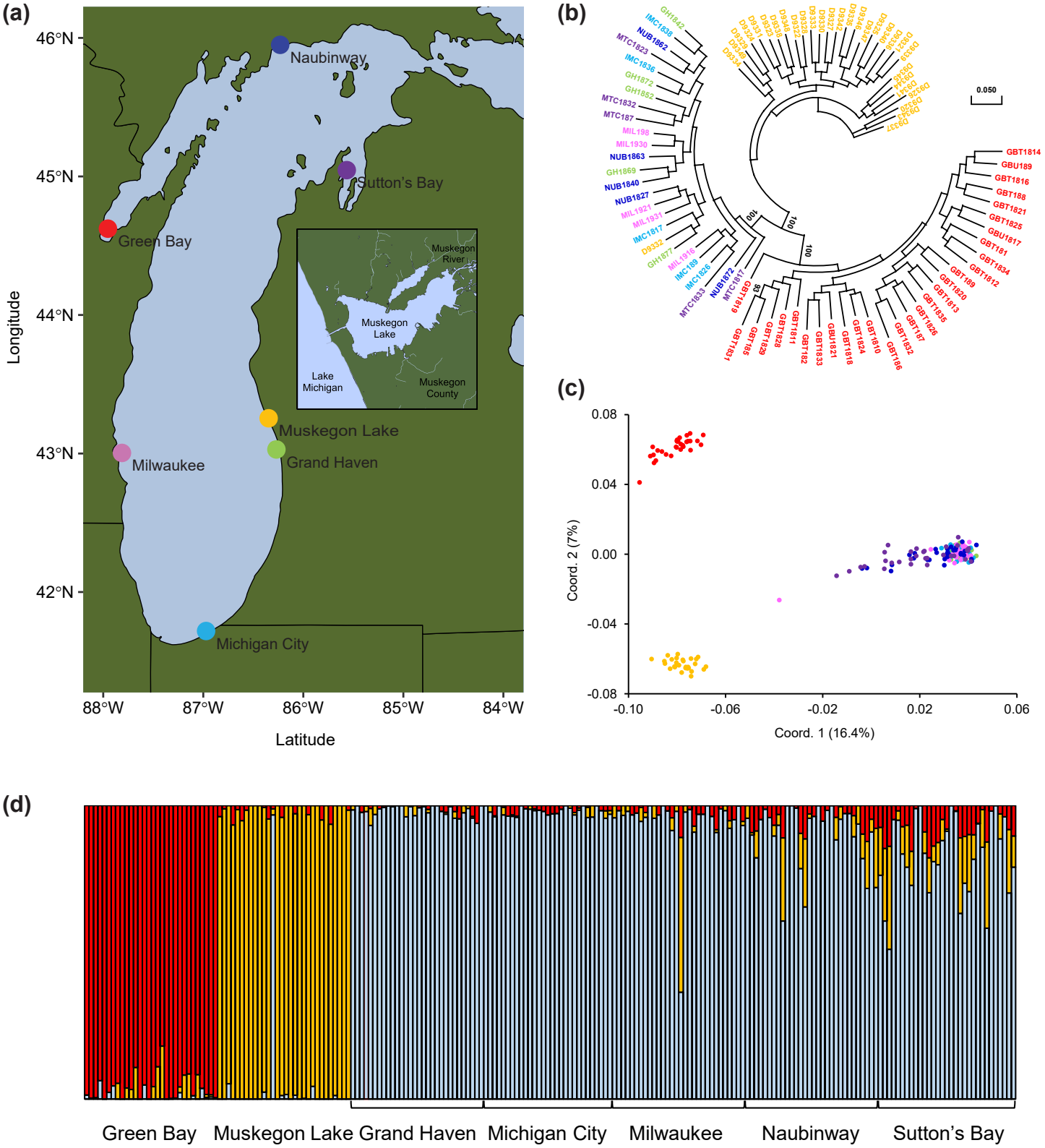
(a)
46°N
45°N
44°N
43°N
42°N
Longitude
88°W
87°W
86°W
85°W
84°W
Latitude
Naubinway
Sutton's Bay
Green Bay
Muskegon Lake
Grand Haven
Milwaukee
Michigan City
Muskegon River
Muskegon Lake
Lake Michigan
Muskegon County
(b)
0.050
100
100
100
53
(c)
0.08
0.04
0.00
-0.04
-0.08
Coord. 2 (7%)
-0.10
-0.06
-0.02
0.02
0.06
Coord. 1 (16.4%)
(d)
Green Bay
Muskegon Lake
Grand Haven
Michigan City
Milwaukee
Naubinway
Sutton's Bay

Figure 2

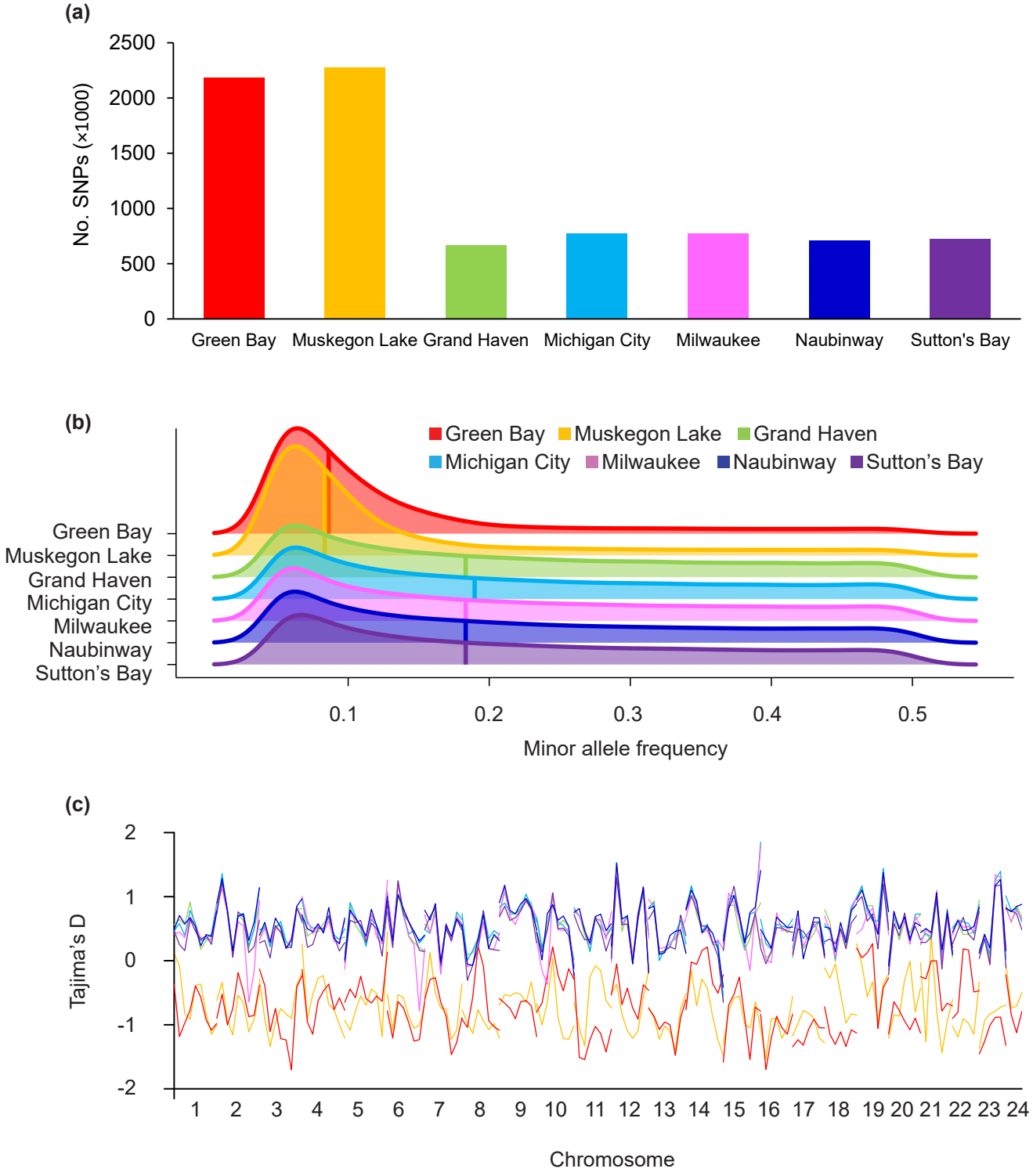
(a)
No. SNPs (×1000)
2500
2000
1500
1000
500
0
Green Bay
Muskegon Lake
Grand Haven
Michigan City
Milwaukee
Naubinway
Sutton's Bay
(b)
Green Bay
Muskegon Lake
Grand Haven
Michigan City
Milwaukee
Naubinway
Sutton's Bay
0.1
0.2
0.3
0.4
0.5
Minor allele frequency
(c)
Tajima's D
2
1
0
-1
-2
1 2 3 4 5 6 7 8 9 10 11 12 13 14 15 16 17 18 19 20 21 22 23 24
Chromosome

Figure 3

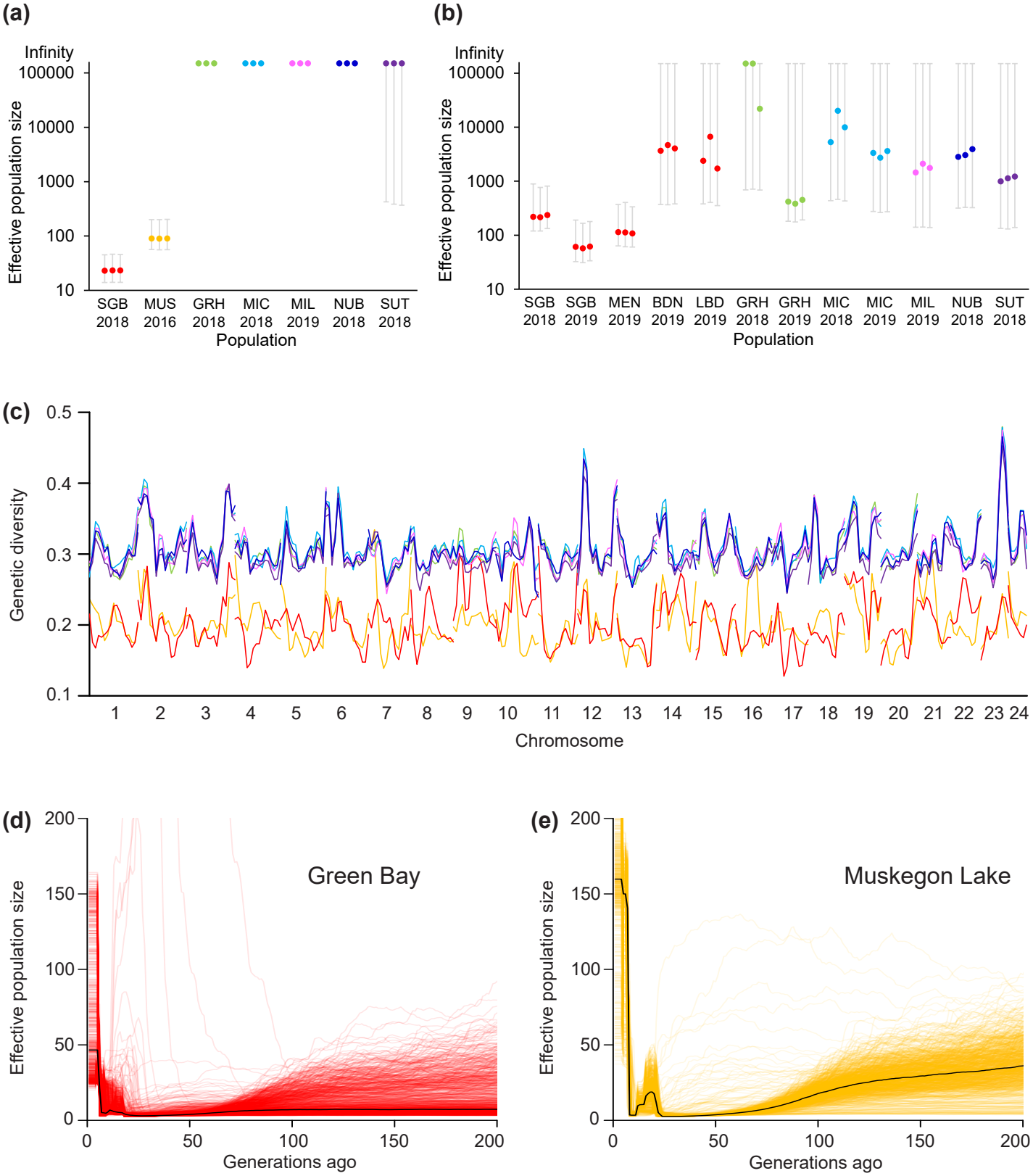
(a)
Infinity
100000
10000
1000
100
10
Effective population size
SGB 2018
MUS 2016
GRH 2018
MIC 2018
MIL 2019
NUB 2018
SUT 2018
Population
(b)
Infinity
100000
10000
1000
100
10
Effective population size
SGB 2018
SGB 2019
MEN 2019
BDN 2019
LBD 2019
GRH 2018
GRH 2019
MIC 2018
MIC 2019
MIL 2019
NUB 2018
SUT 2018
Population
(c)
0.5
0.4
0.3
0.2
0.1
Genetic diversity
1 2 3 4 5 6 7 8 9 10 11 12 13 14 15 16 17 18 19 20 21 22 23 24
Chromosome
(d)
Green Bay
200
150
100
50
0
Effective population size
0 50 100 150 200
Generations ago
(e)
Muskegon Lake
200
150
100
50
0
Effective population size
0 50 100 150 200
Generations ago

Figure 4

(a)

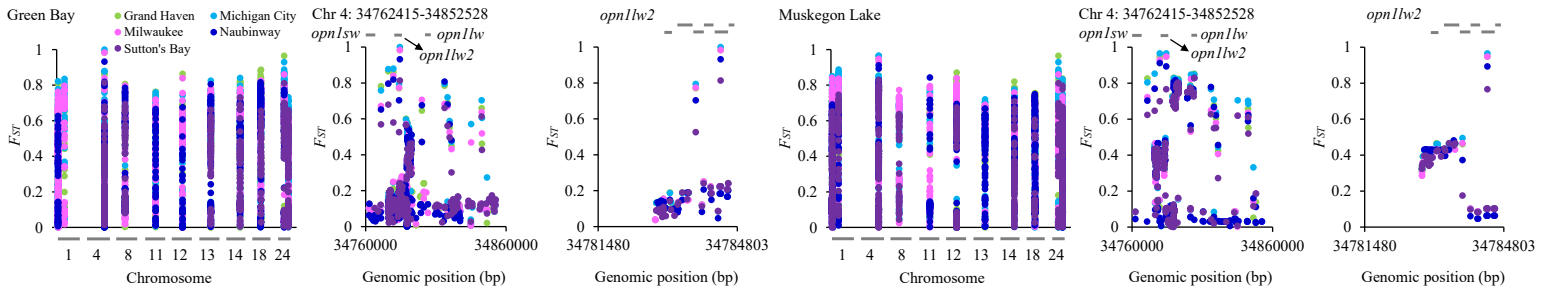

(b)

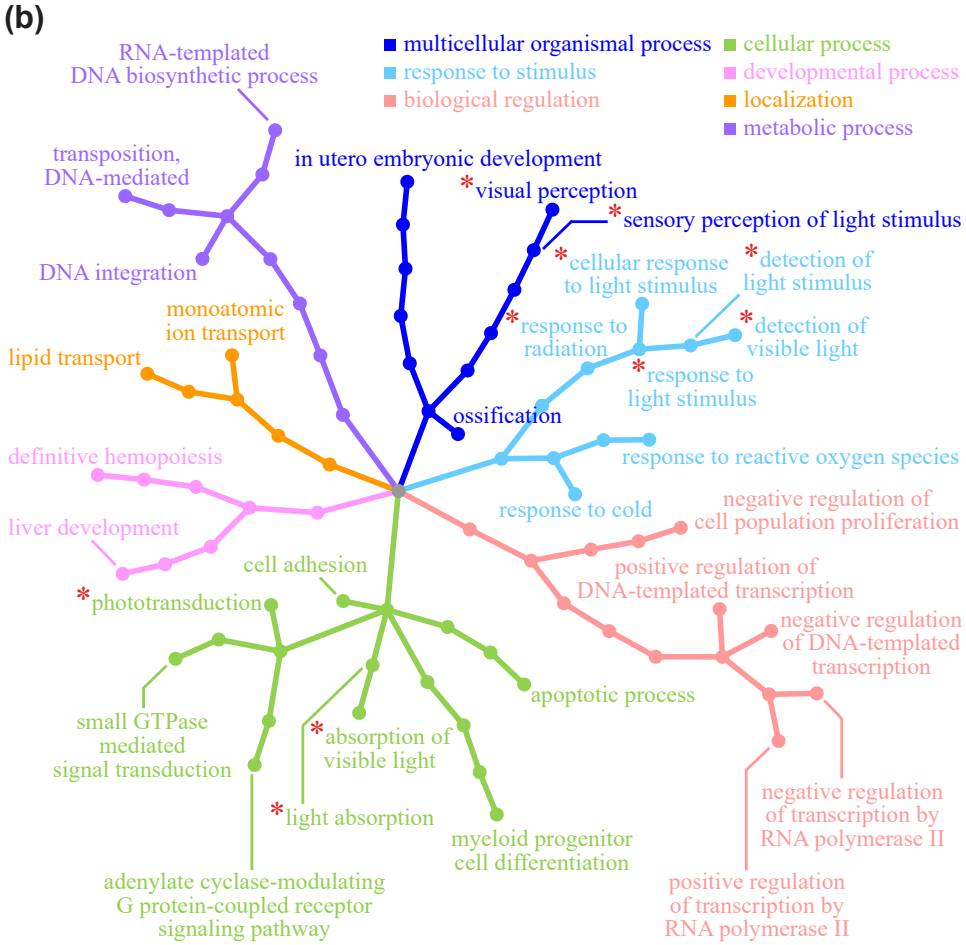

(c)

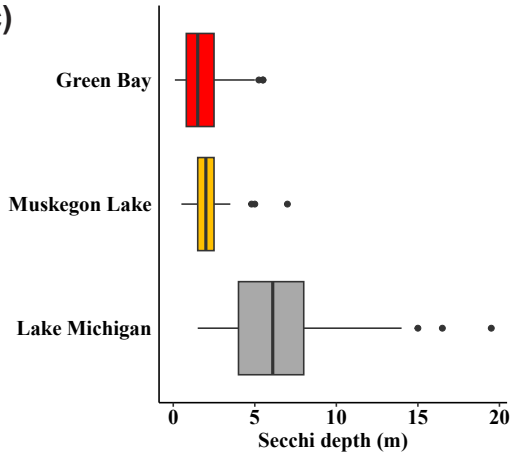

(d)

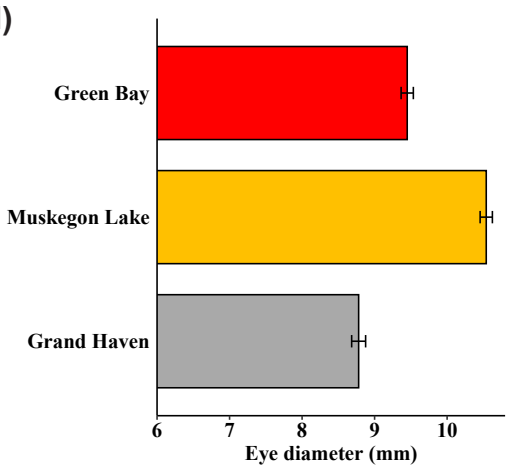

Supplementary Materials for: Rapid, simultaneous increases in the effective sizes of adaptively divergent yellow perch (*Perca flavescens*) populations

Supplementary Methods:

Whole-genome sequencing

We first extracted DNA from 210 yellow perch collected from seven sample sites in Lake Michigan (Supplementary Table 1) using QIAGEN DNeasy® Blood & Tissue Kits. We tested DNA degradation and potential contamination by running agarose gel electrophoresis and quantified DNA concentration using Qubit 2.0. Genomic DNA was fragmented to an average of ~350 bp through sonication. DNA fragments were then end-polished, A-tailed, and ligated with full-length adapters of Illumina sequencing. We amplified the ligated products with P5 and indexed P7 oligos through PCR, purified PCR products using AMPure XP system, checked the size distribution of libraries by Agilent 2100 Bioanalyzer (Agilent Technologies, CA, US), and quantified the libraries using real-time PCR. The libraries were sequenced on an Illumina Novaseq 6000 (Illumina Inc., San Diego, CA, USA) to generate 150 bp paired-end reads. Q20 and Q30 (*i.e.*, the base count of Phred values greater than 20 and 30, respectively, divided by the total base counts) ranged from 94.82%-97.32% and 88%-93.12% of all reads, respectively.

Variant calling and filtering

We called variants following the pipeline "Germline short variant discovery (SNPs + Indels)" provided by the Genome Analysis Toolkit 4.1.9.0 (GATK 4.1.9.0)(1). The DNA sequencing (DNA-Seq) reads were first mapped to the yellow perch genome(2) using BWA-MEM, BAM files were converted into SAM files sorted by query name using Picard tools, and duplicates were marked using the GATK tool, MarkDuplicatesSpark. Next, we called variants per sample

using the GATK tool, HaplotypeCaller, in which we set -ERC to GVCF, --max-alternate-alleles to 100 and --max-num-haplotypes-in-population to 256. Lastly, the GVCF files generated from HaplotypeCaller across all 210 samples were consolidated by chromosome using the GATK tool, GenomicsDBImport, and joint genotyping was conducted using the GATK tool, GenotypeGVCFs, by setting --max-alternate-alleles to 100. We filtered variants using the GATK tool, VariantFiltration, by setting -window to 35 and -cluster to 3 and applying filters "FS >30.0" and "QD < 2.0", and removed indels to retain only single nucleotide polymorphisms (SNPs).

We filtered SNPs using VCFtools (0.1.16). To create two sets of SNPs for downstream analyses, we first set genotypes called at loci covered by fewer than three reads in each sample as missing values by setting --minDP to 3, deleted SNPs that were genotyped in fewer than 90% of samples by setting --max-missing-count to 42, kept only biallelic SNPs by setting the flags --max-alleles and --min-alleles to 2, and filtered out SNPs with minor allele frequency (MAF) smaller than 0.05 across 210 samples in all seven sample sites to create the **study-wide** data set. This set of SNPs were used to create phylogenetic trees using RAxML version 8.2.12(3), run principal coordinate analysis using *hierfstat* in R version 4.2.1(4) and GenAlEx 6.51b2(5), and conduct population structure analysis on all sample groups using Admixture 1.3(6) (Supplementary Table 3). Second, we split the VCF file with SNPs by sample site into seven separate VCF files, one for each sample site, set genotypes called at loci covered by fewer than three reads in each sample as missing values by setting --minDP to 3, deleted SNPs that were genotyped in fewer than 90% of samples by setting --max-missing-count to 5 (for Michigan City) or 6 (for the other six sample sites) due to different sample sizes of seven sample sites (Supplementary Table 1), kept only biallelic SNPs by setting the flags --max-alleles and --min-alleles to 2, and filtered SNPs by MAF for each population by discarding SNPs that have MAF

smaller than 0.02 or 0.05 within each population to create the **within-group** data sets. The set of SNPs filtered by MAF ≥ 0.02 were used to calculate Tajima's D using VCFtools (0.1.16), while the set of SNPs filtered by MAF ≥ 0.05 were used to assess minor allele frequency distributions, calculate genetic diversity (*i.e.*, observed heterozygosity), estimate effective population size using NeEstimator V2(7), and reconstruct demographic histories using GONE(8) (Supplementary Table 3).

Supplementary Results:

Genetic divergence among yellow perch sample sites

The high genetic divergence between Green Bay and main basin sample sites, as revealed by Miller(9) and Schraidt et al.(10), could be driven by the limited larval exchange between the two basins(11). One sample collected from Muskegon Lake (sample id: D9332) in July 2016 clustered with main basin sample sites, suggesting that migration between the main basin and Muskegon Lake is possible. Interestingly, D9332 was captured via a nighttime boat electrofishing survey at the State Park site in Muskegon Lake (see Fig. 1 in Bhagat and Ruetz(12)), which is closest to Lake Michigan among the four sites we sampled in Muskegon Lake. Additionally, D9332 was 10.4 cm TL, which was smaller than the mean size of yellow perch in Muskegon Lake (mean = 15.5 cm TL). Therefore, D9332 was likely born in the main basin of Lake Michigan and subsequently moved into Muskegon Lake. The movement of yellow perch from the main basin into Muskegon Lake has been suggested previously by Chorak et al.(13,14). Despite the clear movement of a single individual, we found the remaining Muskegon Lake samples to be genetically divergent from main basin sample sites (Fig. 1b,d; see Supplementary Table 5 for all pairwise F_{ST} estimates).

Life history of yellow perch

Yellow perch have a bipartite life cycle consisting of a dispersive larval stage of 30 to 40 days(15,16), followed by demersal, relatively site-attached juveniles and adult life stages(10,17). Adult yellow perch exhibits relatively high site fidelity to spawning grounds(17–19). Female yellow perch lay their eggs in skeins(20) and, after about 15-20 days of egg development in Lake Michigan, embryos hatch into minuscule larvae, which disperse passively in the currents for approximately 30-40 days during their early life stages and may eventually adopt a strategy of combined active and passive dispersal as larvae develop and perform better at swimming(21). Similar to many marine fishes, yellow perch have high fecundity, high larval and juvenile mortality, and large population sizes(22–24).

Supplementary Discussion:

We found a strong relationship between decreases in nutrient loads and concomitant increases in *Ne* in two geographically separated yellow perch populations (Supplementary Fig. 9, Supplementary Fig. 10). While we are aware that correlation does not equal causation, we speculate that this result may suggest that improvements in water quality can result in increased *Ne*. Water quality in Green Bay and Muskegon Lake was at its worst in the early 1970s, after which environmental remediation resulted in substantial water quality and habitat improvements, particularly for reductions in phosphorus(25,26) (Supplementary Fig. 9). Given an estimated generation time of 4 years(22,27), effective population sizes of yellow perch populations began rebounding in the early 2000s, some 20-30 years after cleanup efforts were well under way (generation time estimates of 3 and 5 years show similar results; Supplementary Fig. 9b; Supplementary Fig. 10). For both Green Bay and Muskegon Lake, there is a strong relationship between total phosphorous and effective population size (Supplementary Fig. 9c), suggesting

that, as nutrient loading decreased, *Ne* increased (but see caveats below). Note that while more data on phosphorus were available for Muskegon Lake due to the use of sediment cores to quantify changes through time, concentrations of phosphorus and other nutrients also have declined in Green Bay since the 1970s(25).

Mismatches may exist between *Ne* estimated by GONE and actual abundances obtained from fishery dependent or independent surveys in some populations. Historical data on catch rate per unit effort (CPUE) suggests that abundance of yellow perch in Green Bay started increasing since late 1970s and peaked around 1980s(28), while *Ne* of the Green Bay site we sampled remained relatively low through 1970s and 1980s, started increasing around 1990s, and reached maximum around 2000 (Supplementary Fig. 9, Supplementary Fig. 10). There are several potential explanations for this mismatch. First, the timing of major historical events estimated by GONE may not be accurate. Although GONE is fairly robust to genotyping errors, temporal heterogeneity of samples, population admixture, and population subdivision, biases arising from violations of isolation and panmixia of populations under study may not be fully eliminated(8,29). Second, overlapping generations and fishing-induced evolution may both complicate the estimation of generation times, leading to incorrect conversion from generation, which is output along with *Ne* by GONE, into specific time points. Third, slight differences in *Ne* are detected across sample sites in Green Bay (Fig. 3b), so the reconstructed demographic history for our collection site may not be representative of *Ne* of the entire region and thus may not be representative for all of Green Bay. Lastly, current methods for estimating fish abundance are also not free of bias. CPUE may not be a reliable estimator for stock abundance because: 1.) the correlation between commercial catch rates and stock abundance may not hold due to aggregated fishing, undocumented changes in fishing efforts, differential proportions of species captured,

and by-catch discard(30–33), and 2.) insufficient time series of data, owing to the difficulty in data collection over a large temporal scale, may reduce confidence in model predictions(34).

References

1. McKenna A, Hanna M, Banks E, Sivachenko A, Cibulskis K, Kernytsky A, et al. The Genome Analysis Toolkit: A MapReduce framework for analyzing next-generation DNA sequencing data. Genome Res. 2010 Sep;20(9):1297–303.

2. Feron R, Zahm M, Cabau C, Klopp C, Roques C, Bouchez O, et al. Characterization of a Y-specific duplication/insertion of the anti-Mullerian hormone type II receptor gene based on a chromosome-scale genome assembly of yellow perch, *Perca flavescens*. Molecular Ecology Resources [Internet]. 2020 [cited 2022 Jul 14];20(2):531–43. Available from: https://onlinelibrary.wiley.com/doi/abs/10.1111/1755-0998.13133

3. Stamatakis A. RAxML version 8: a tool for phylogenetic analysis and post-analysis of large phylogenies. Bioinformatics. 2014 May 1;30(9):1312–3.

4. R Core Team. R: A language and environment for statistical computing. R Foundation for Statistical Computing, Vienna, Austria. URL https://www.R-project.org/. 2020;

5. Peakall R, Smouse PE. GenAlEx 6.5: genetic analysis in Excel. Population genetic software for teaching and research—an update. Bioinformatics [Internet]. 2012 Oct 1 [cited 2022 Aug 12];28(19):2537–9. Available from: https://www.ncbi.nlm.nih.gov/pmc/articles/PMC3463245/

6. Alexander DH, Novembre J, Lange K. Fast model-based estimation of ancestry in unrelated individuals. Genome Res. 2009 Sep;19(9):1655–64.

7. Do C, Waples RS, Peel D, Macbeth GM, Tillett BJ, Ovenden JR. NeEstimator v2: re-implementation of software for the estimation of contemporary effective population size (*Ne*) from genetic data. Molecular Ecology Resources [Internet]. 2014 [cited 2022 Jul 14];14(1):209–14. Available from: https://onlinelibrary.wiley.com/doi/abs/10.1111/1755-0998.12157

8. Santiago E, Novo I, Pardiñas AF, Saura M, Wang J, Caballero A. Recent demographic history inferred by high-resolution analysis of linkage disequilibrium. Molecular Biology and Evolution [Internet]. 2020 Dec 16 [cited 2022 Sep 17];37(12):3642–53. Available from: https://doi.org/10.1093/molbev/msaa169

9. Miller LM. Microsatellite DNA loci reveal genetic structure of yellow perch in Lake Michigan. Transactions of the American Fisheries Society [Internet]. 2003 [cited 2022 Oct 31];132(3):503–13. Available from: https://onlinelibrary.wiley.com/doi/abs/10.1577/1548-8659%282003%29132%3C0503%3AMDLRGS%3E2.0.CO%3B2

10. Schraidt CE, Ackiss AS, Larson WA, Rowe MD, Höök TO, Christie MR. Dispersive currents explain patterns of population connectivity in an ecologically and economically important fish. Evolutionary Applications [Internet]. 2023 [cited 2023 Sep 10];16(7):1284–301. Available from: https://onlinelibrary.wiley.com/doi/abs/10.1111/eva.13567

11. Beletsky D, Schwab DJ. Modeling circulation and thermal structure in Lake Michigan: Annual cycle and interannual variability. Journal of Geophysical Research: Oceans [Internet]. 2001 [cited 2022 Aug 13];106(C9):19745–71. Available from: https://onlinelibrary.wiley.com/doi/abs/10.1029/2000JC000691

12. Bhagat Y, Ruetz III CR. Temporal and fine-scale spatial variation in fish assemblage structure in a drowned river mouth system of Lake Michigan. Transactions of the American Fisheries Society [Internet]. 2011 [cited 2022 Oct 29];140(6):1429–40. Available from: https://onlinelibrary.wiley.com/doi/abs/10.1080/00028487.2011.630278

13. Chorak GM, Ruetz III CR, Thum RA, Partridge CG, Janetski DJ, Höök TO, et al. Yellow perch genetic structure and habitat use among connected habitats in eastern Lake Michigan. Ecology and Evolution [Internet]. 2019 [cited 2022 Aug 13];9(16):8922–32. Available from: https://onlinelibrary.wiley.com/doi/abs/10.1002/ece3.5219

14. Senegal TJ, Ruetz CR, Chorak GM, Janetski DJ, Clapp DF, Bowen GJ, et al. Differential habitat use patterns of yellow perch *Perca flavescens* in eastern Lake Michigan and connected drowned river mouth lakes. Journal of Great Lakes Research [Internet]. 2020 Oct 1 [cited 2022 Oct 31];46(5):1412–22. Available from: https://www.sciencedirect.com/science/article/pii/S038013302030143X

15. Whiteside MC, Swindoll CM, Doolittle WL. Factors affecting the early life history of yellow perch, *Perca flavescens*. Environ Biol Fish [Internet]. 1985 Jan 1 [cited 2022 Aug 15];12(1):47–56. Available from: https://doi.org/10.1007/BF00007709

16. Dettmers JM, Janssen J, Pientka B, Fulford RS, Jude DJ. Evidence across multiple scales for offshore transport of yellow perch (*Perca flavescens*) larvae in Lake Michigan. Can J Fish Aquat Sci [Internet]. 2005 Dec [cited 2022 Aug 15];62(12):2683–93. Available from: https://cdnsciencepub.com/doi/10.1139/f05-173

17. Glover DC, Dettmers JM, Wahl DH, Clapp DF. Yellow perch (*Perca flavescens*) stock structure in Lake Michigan: an analysis using mark–recapture data. Can J Fish Aquat Sci [Internet]. 2008 Sep [cited 2022 Aug 15];65(9):1919–30. Available from: https://cdnsciencepub.com/doi/10.1139/F08-100

18. Bohling P, Lehtonen H. Effect of environmental factors on migrations of perch (*Perca fluviatilis* L.) tagged in the coastal waters of Finland. Finnish Fisheries Research. 1984;5:31–40.

19. Schneeberger PJ. Population dynamics of contemporary yellow perch and walleye stocks in Michigan waters of Green Bay, Lake Michigan, 1988-96. Dept. of Natural Resources, Fisheries Division; 2000.

20. Robillard SR, Marsden JE. Spawning substrate preferences of yellow perch along a sand–cobble shoreline in southwestern Lake Michigan. North American Journal of Fisheries Management [Internet]. 2001 Feb 1 [cited 2022 Aug 15];21(1):208–15. Available from: https://doi.org/10.1577/1548-8675(2001)021<0208:SSPOYP>2.0.CO;2

21. Beletsky D, Mason DM, Schwab DJ, Rutherford ES, Janssen J, Clapp DF, et al. Biophysical model of larval yellow perch advection and settlement in Lake Michigan. Journal of Great Lakes Research [Internet]. 2007 Jan 1 [cited 2022 Aug 15];33(4):842–66. Available from: https://www.sciencedirect.com/science/article/pii/S0380133007701028

22. Brazo D, Tack P, Liston C. Age, growth, and fecundity of yellow perch, *Perca flavescens*, in Lake Michigan near Ludington, Michigan. Transactions of the American Fisheries Society. 1975;104(4):726–30.

23. Ludsin SA, DeVanna KM, Smith REH. Physical–biological coupling and the challenge of understanding fish recruitment in freshwater lakes. Can J Fish Aquat Sci. 2014;71(5):775–94.

24. Pritt JJ, Roseman EF, O'Brien TP. Mechanisms driving recruitment variability in fish: comparisons between the Laurentian Great Lakes and marine systems. ICES Journal of Marine Science [Internet]. 2014 Oct 1 [cited 2022 Aug 15];71(8):2252–67. Available from: https://doi.org/10.1093/icesjms/fsu080

25. Harris HJ, Wenger RB, Sager PE, Val Klump J. The Green Bay saga: Environmental change, scientific investigation, and watershed management. Journal of Great Lakes Research [Internet]. 2018 Oct 1 [cited 2023 Sep 24];44(5):829–36. Available from: https://www.sciencedirect.com/science/article/pii/S0380133018301412

26. Liu B, McLean CE, Long DT, Steinman AD, Stevenson RJ. Eutrophication and recovery of a lake inferred from sedimentary diatoms originating from different habitats. Science of The Total Environment [Internet]. 2018 Jul 1 [cited 2023 Sep 24];628–629:1352–61. Available from: https://www.sciencedirect.com/science/article/pii/S0048969718305679

27. Hart S, Garling D, Malison J. Yellow perch (*Perca flavescens*) culture guide. North Central Regional Aquaculture Center. 2006;

28. Clapp D, Makauskas D. Status of yellow perch in Lake Michigan - 2019-2020. Report to the Lake Michigan committee. 2021;

29. Novo I, Ordás P, Moraga N, Santiago E, Quesada H, Caballero A. Impact of population structure in the estimation of recent historical effective population size by the software GONE. Genet Sel Evol [Internet]. 2023 Dec 4 [cited 2024 Feb 27];55(1):86. Available from: https://doi.org/10.1186/s12711-023-00859-2

30. Marchal P, Andersen B, Caillart B, Eigaard O, Guyader O, Hovgaard H, et al. Impact of technological creep on fishing effort and fishing mortality, for a selection of European fleets. ICES Journal of Marine Science [Internet]. 2007 Jan 1 [cited 2024 Feb 27];64(1):192–209. Available from: https://doi.org/10.1093/icesjms/fsl014

31. O'Neill MF, Leigh GM. Fishing power increases continue in Queensland's east coast trawl fishery, Australia. Fisheries Research [Internet]. 2007 Jun 1 [cited 2024 Feb 27];85(1):84–92. Available from: https://www.sciencedirect.com/science/article/pii/S0165783607000057

32. Branch TA, Hilborn R. Matching catches to quotas in a multispecies trawl fishery: targeting and avoidance behavior under individual transferable quotas. Can J Fish Aquat Sci [Internet]. 2008 Jul [cited 2024 Feb 27];65(7):1435–46. Available from: https://cdnsciencepub.com/doi/full/10.1139/F08-065

33. Winker H, Kerwath SE, Attwood CG. Comparison of two approaches to standardize catch-per-unit-effort for targeting behaviour in a multispecies hand-line fishery. Fisheries Research [Internet]. 2013 Mar 1 [cited 2024 Feb 27];139:118–31. Available from: https://www.sciencedirect.com/science/article/pii/S0165783612003311

34. Ovenden JR, Leigh GM, Blower DC, Jones AT, Moore A, Bustamante C, et al. Can estimates of genetic effective population size contribute to fisheries stock assessments? Journal of Fish Biology [Internet]. 2016 [cited 2024 Feb 11];89(6):2505–18. Available from: https://onlinelibrary.wiley.com/doi/abs/10.1111/jfb.13129

35. Sparks MM, Schraidt CE, Yin X, Seeb LW, Christie MR. Rapid genetic adaptation to a novel ecosystem despite a large founder event. Mol Ecol. 2023 Sep 5;

36. Liu X, Fu YX. Stairway Plot 2: demographic history inference with folded SNP frequency spectra. Genome Biology [Internet]. 2020 Nov 17 [cited 2022 Jul 14];21(1):280. Available from: https://doi.org/10.1186/s13059-020-02196-9

37. Wigginton JE, Cutler DJ, Abecasis GR. A note on exact tests of Hardy-Weinberg equilibrium. Am J Hum Genet. 2005 May;76(5):887–93.

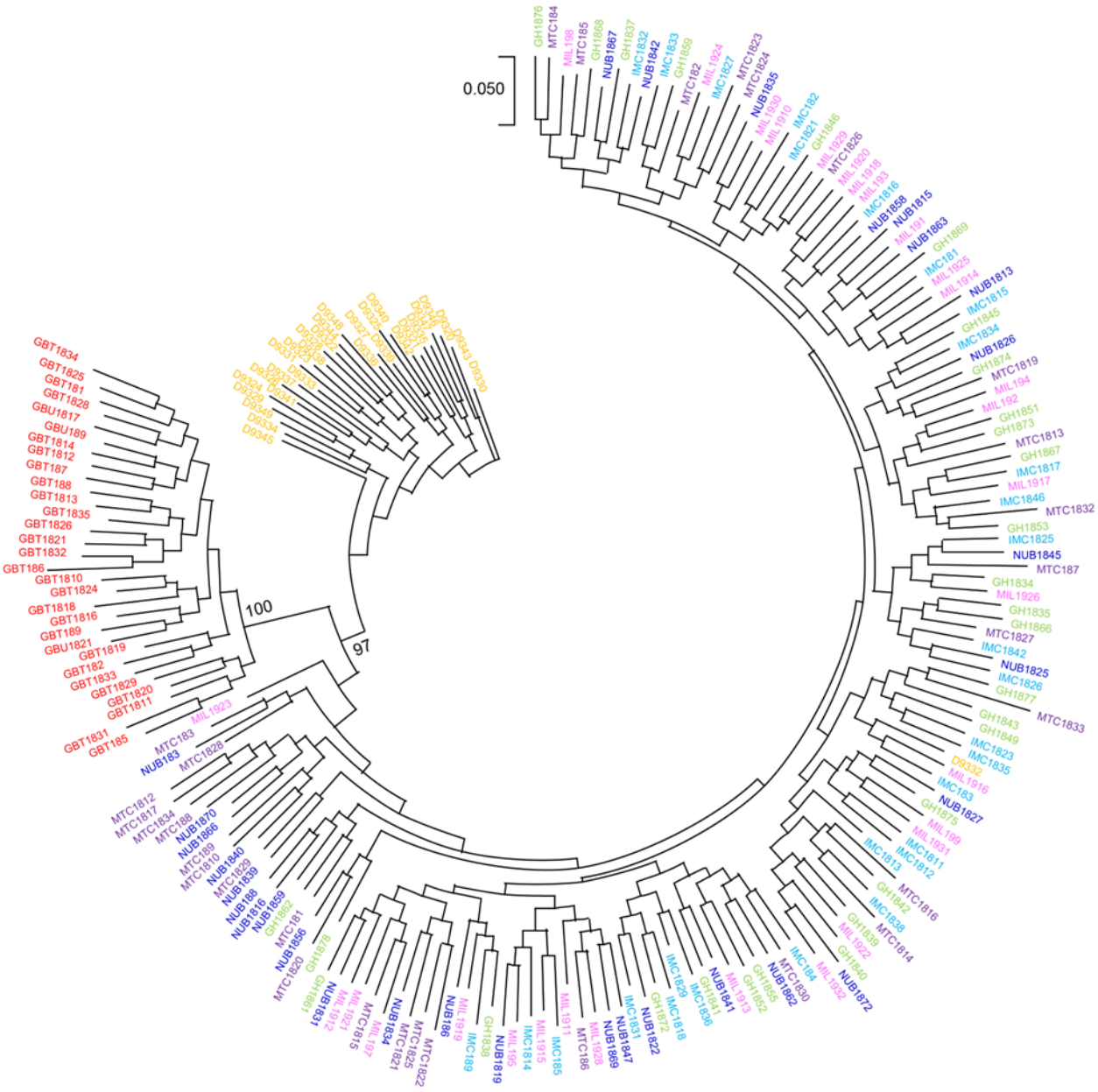

● Green Bay ● Muskegon Lake ● Grand Haven ● Michigan City ● Milwaukee ● Naubinway ● Sutton's Bay

Supplementary Figure 1. Phylogenetic tree for all 210 samples. The phylogenetic tree was constructed with 5,000 randomly selected SNPs from all 210 samples using RAxML version 8.2.12(3). Numbers on branches indicate the percentage of bootstraps returning the best-scoring ML tree in 1,000 alternative runs with distinct starting trees and values are only shown when greater than 90%.

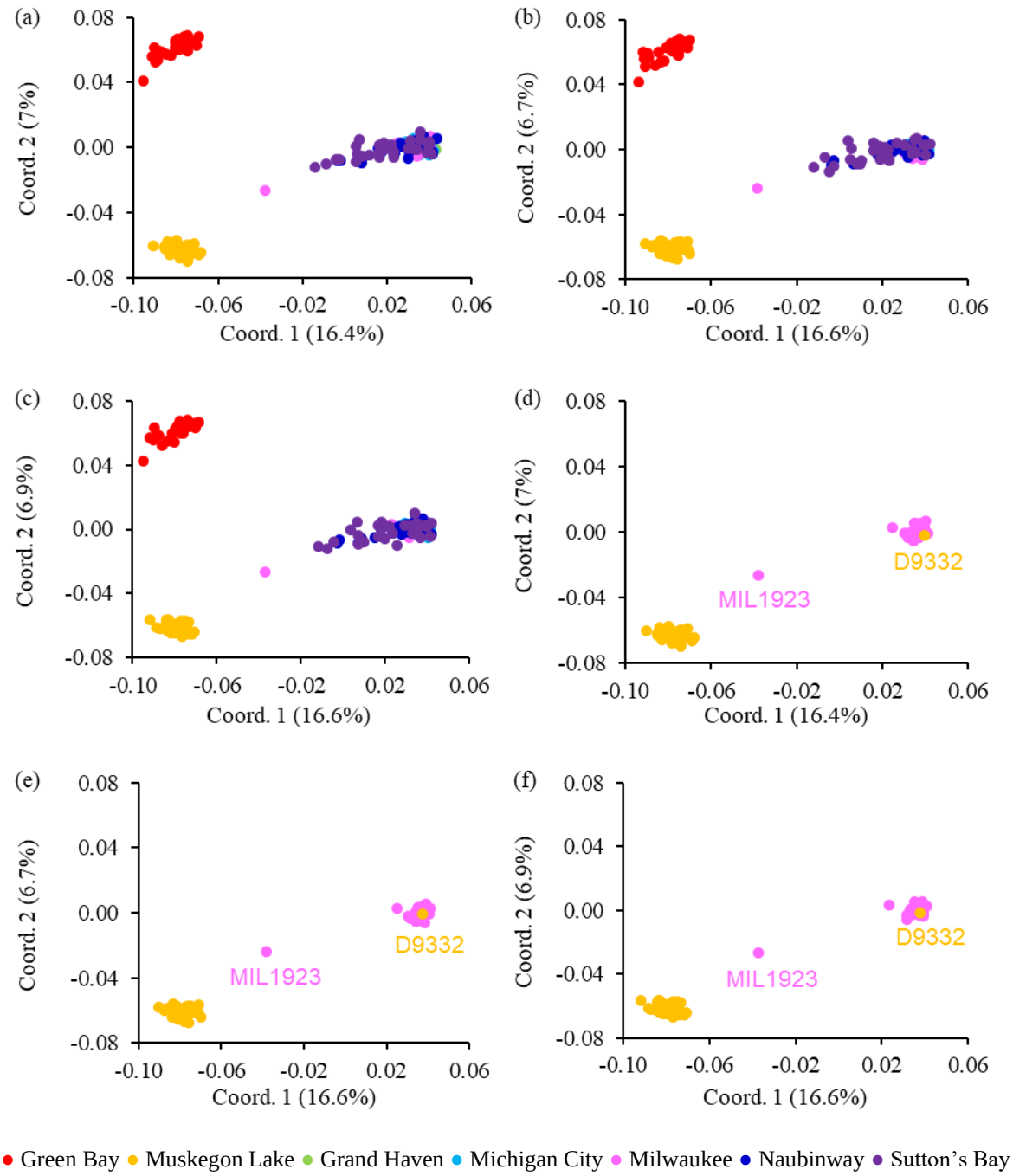

Supplementary Figure 2. Principal coordinate analysis using *hierfstat* in R version 4.2.1 for all seven sample sites (a, b, c) and Muskegon Lake and Milwaukee (d, e, f). Principal coordinate analysis was conducted independently three times with three different sets of 50,000 randomly selected SNPs to account for the potential variation caused by different SNPs. One Muskegon Lake sample clusters with the main basin populations, suggesting potential migration from the main basin. One Milwaukee sample falls comparatively further away from the main basin populations, suggesting potential gene flow or shared ancestry with a fish of unknown origin. Panel (a) is the same as Fig. 1c in the main text.

(a)

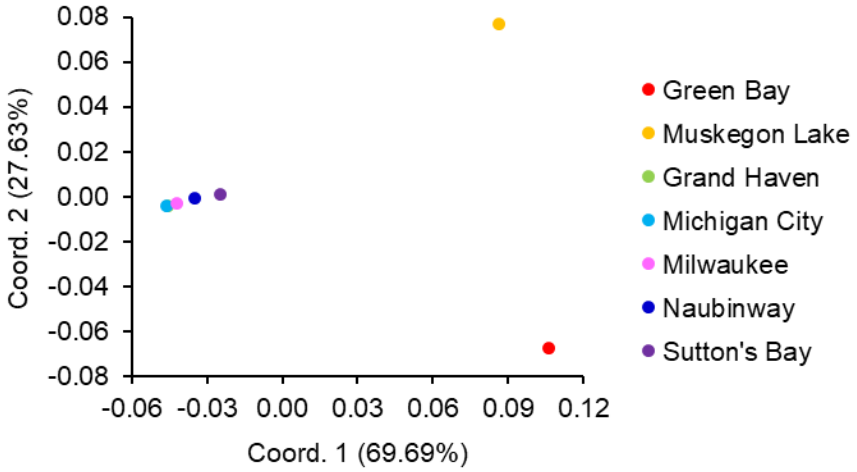

(b)

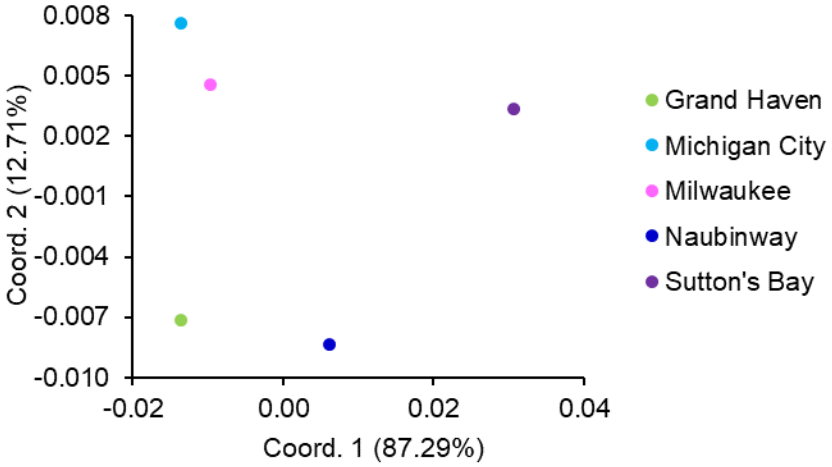

Supplementary Figure 3. Principal coordinate analysis of mean pairwise F_{ST} for all seven sample sites (a) and five main basin sample sites (b) based on mean Weir and Cockerham's F_{ST} between pairs of sample sites (see Supplementary Table 5 for details). Note that the northern main basin sample sites are slightly divergent from the southern main basin sample sites (axis 1 of panel b), a finding congruent with earlier RAD-Seq analyses(10), and Grand Haven is missing in panel (a) because it is hidden behind Michigan City.

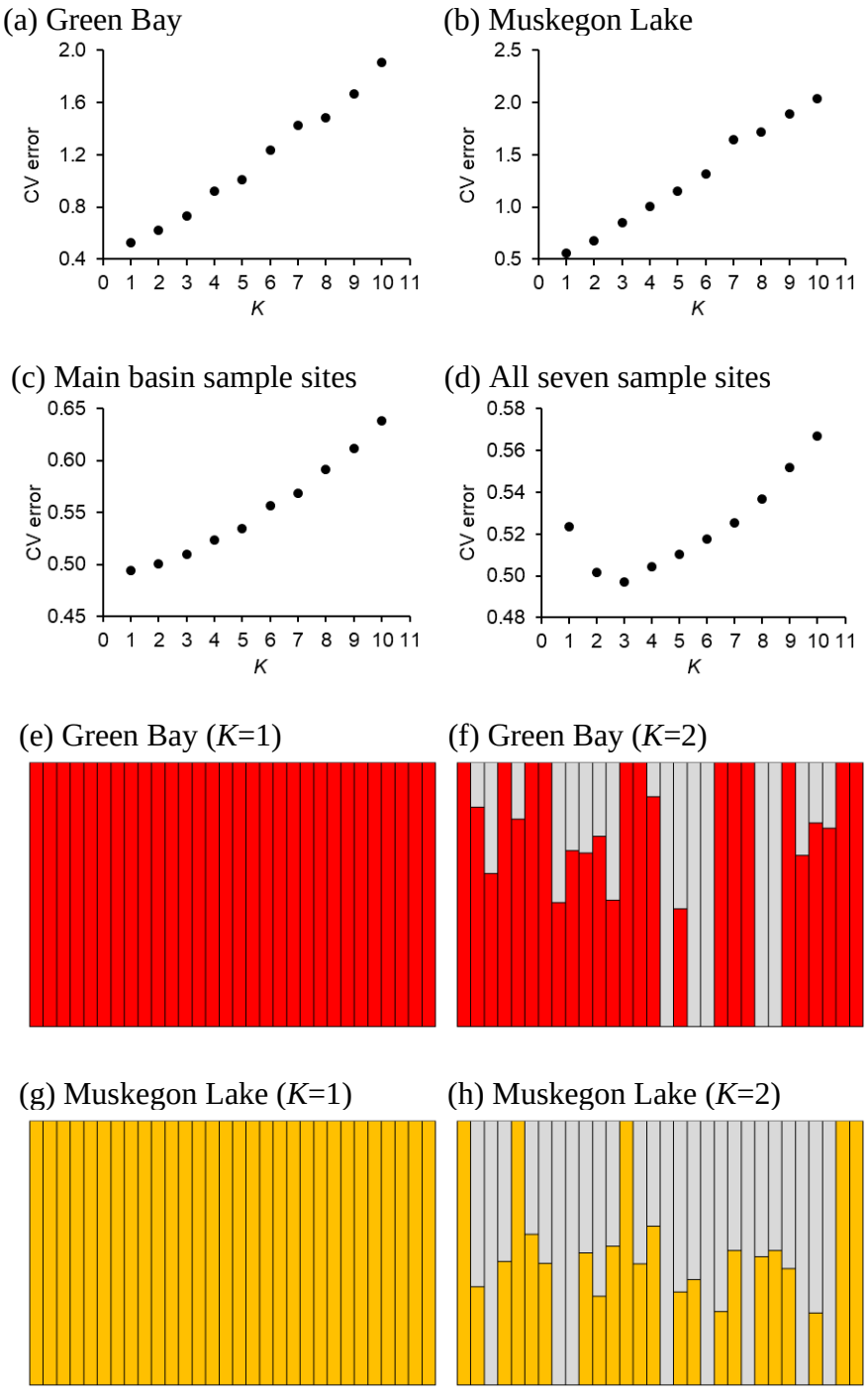

Supplementary Figure 4. Optimal *K* in admixture analysis for Green Bay (a, optimal *K*=1), Muskegon Lake (b, optimal *K*=1), main basin sample sites (c, optimal *K*=1), and all seven sample sites (d, optimal *K*=3) and ancestry plots of Green Bay (e, f) and Muskegon Lake (g, h) populations.

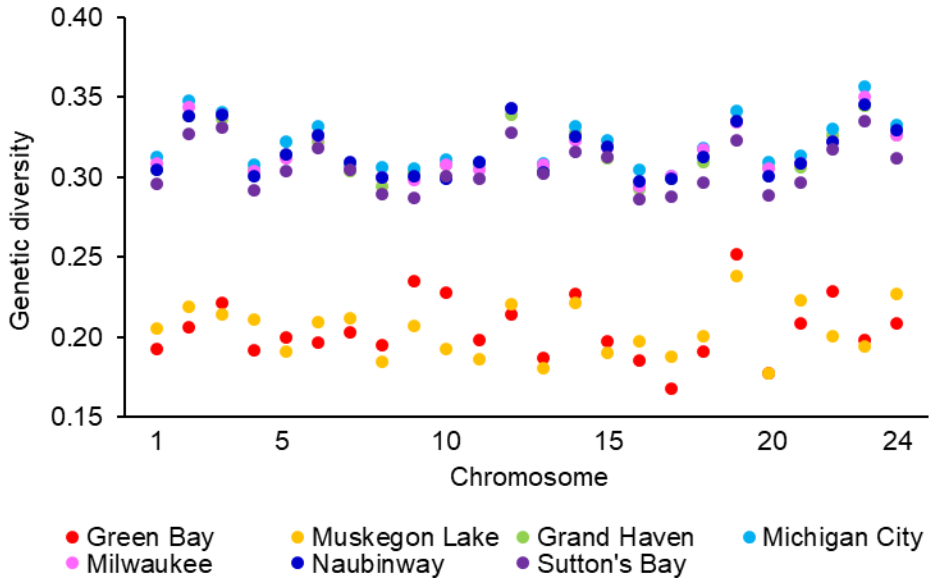

Supplementary Figure 5. Chromosome-level genetic diversity. Observed heterozygosity was calculated as the number of heterozygous individuals divided by the number of genotyped individuals at SNPs from the within-group data set (MAF ≥ 0.05) and averaged across each chromosome.

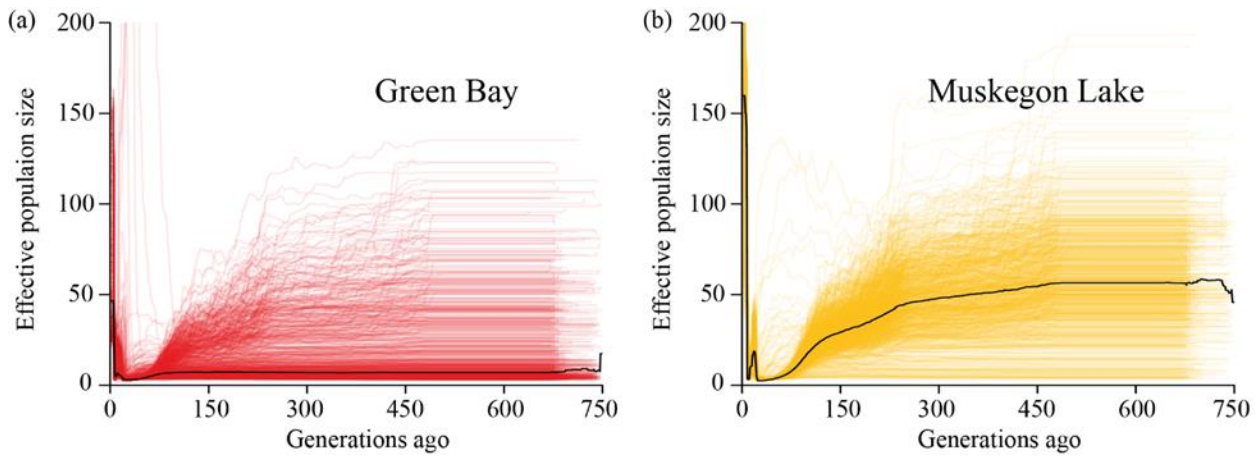

Supplementary Figure 6. Demographic histories of Green Bay (red) and Muskegon Lake (orange) reconstructed with 1,000 replicates of 30,000 SNPs randomly selected from the within-group data set using GONE with a black line indicating median effective population size. In comparison to Fig. 3d,e in the main text, (a) and (b) illustrate the entire demographic inferences of Green Bay and Muskegon Lake over the past 750 generations. Note, however, that GONE is not very accurate in reconstructing demographic histories prior to bottlenecks(35).

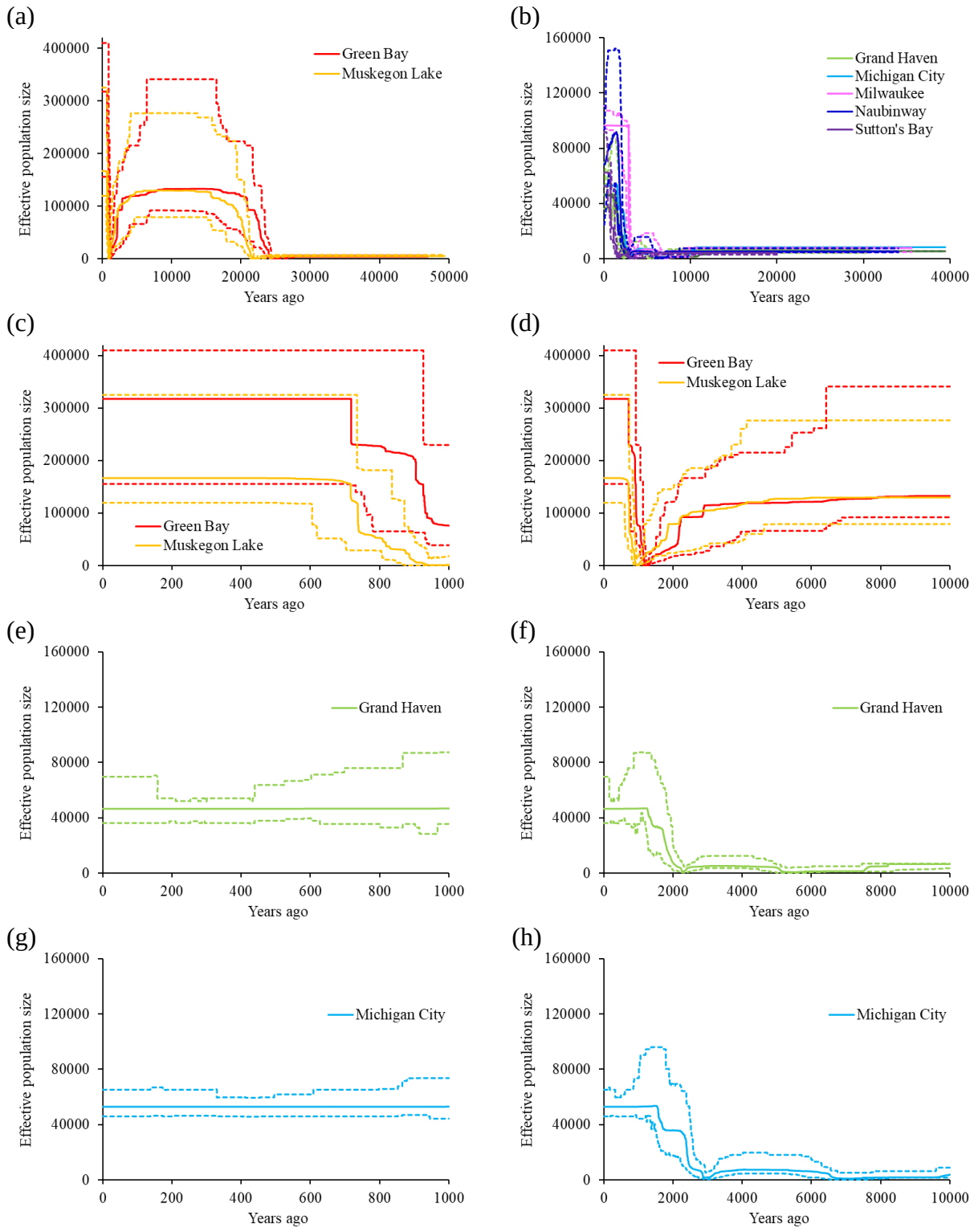
(a)
Green Bay
Muskegon Lake
Effective population size
Years ago
(b)
Grand Haven
Michigan City
Milwaukee
Naubinway
Sutton's Bay
Effective population size
Years ago
(c)
Green Bay
Muskegon Lake
Effective population size
Years ago
(d)
Green Bay
Muskegon Lake
Effective population size
Years ago
(e)
Grand Haven
Effective population size
Years ago
(f)
Grand Haven
Effective population size
Years ago
(g)
Michigan City
Effective population size
Years ago
(h)
Michigan City
Effective population size
Years ago

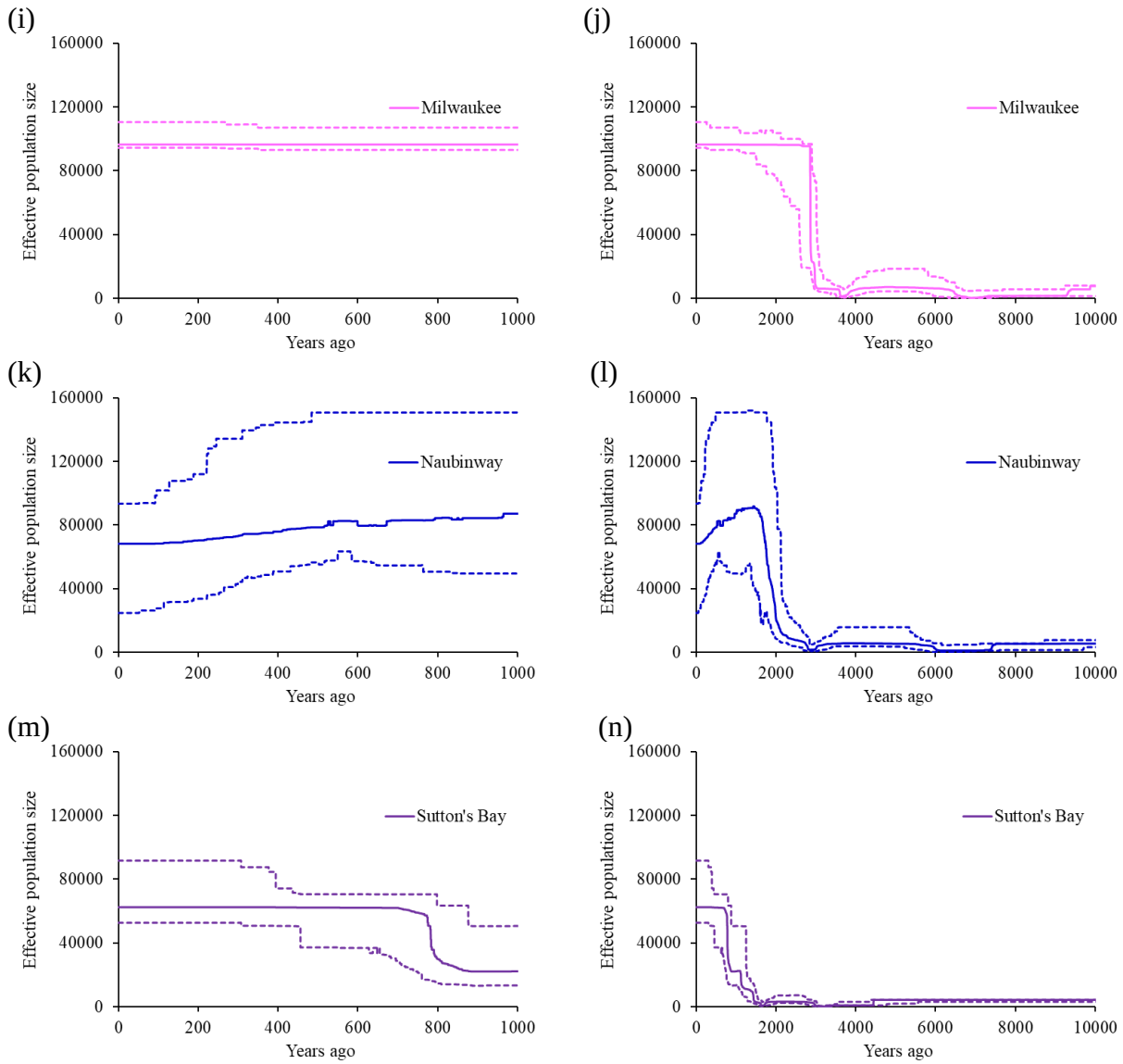

Supplementary Figure 7. Demographic histories reconstructed by Stairway Plot 2(36) with a generation time of 2 years with solid lines indicating median *Ne* and dashed lines indicating 95% CI of *Ne*.

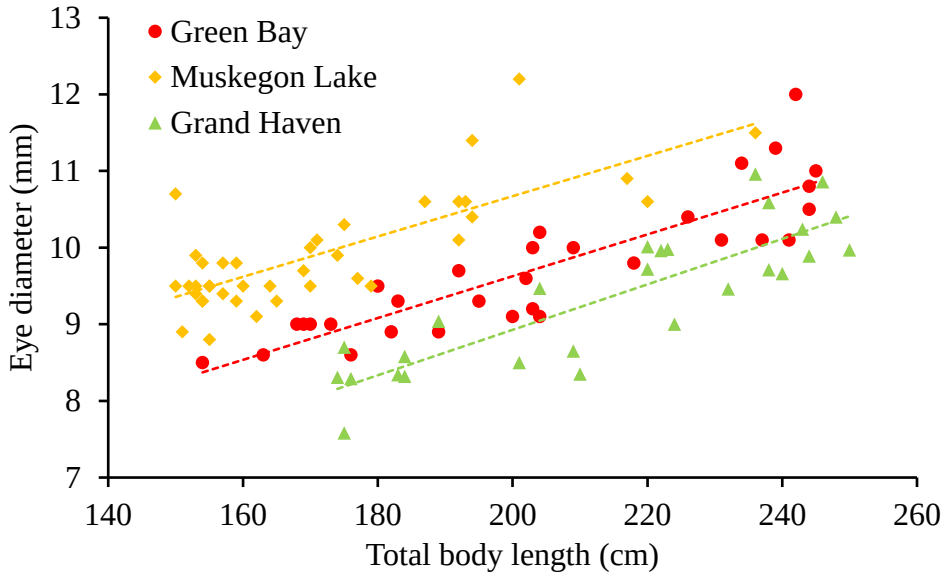

Supplementary Figure 8. Regression of eye diameter (mm) on total body length (cm) of yellow perch collected from Menominee in Green Bay, Muskegon Lake, and Grand Haven (i.e., Lake Michigan main basin). A significant positive relationship is detected between eye diameter and total body length ($P < 0.001$), but slopes of linear regressions of eye diameter on total body length are not significantly different for yellow perch among Green Bay, Muskegon Lake, and Grand Haven ($P = 0.779$).

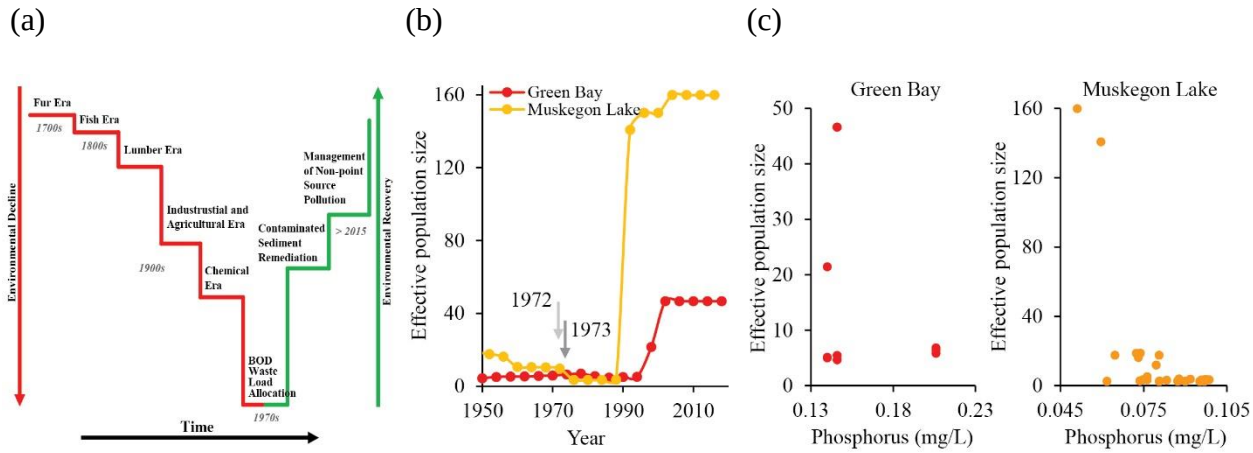

Supplementary Figure 9. Increased effective population size driven by environmental remediation. Environmental conditions deteriorated with industrial development and human population expansion and were subsequently ameliorated, at least in part, by a series of environmental initiatives implemented since the late 1970s (a). Along with the ecosystem restoration driven by environmental initiatives, such as the Clean Water Act since 1972 (indicated with a light gray arrow) and the Muskegon County advanced wastewater treatment since 1973 (indicated with a dark gray arrow), effective population size started rebounding shortly after policies were implemented (b). Increases in effective population sizes are associated with substantial reductions in total phosphorus in both Green Bay and Muskegon Lake (c). Panel a is reproduced from Harris et al. with permission.

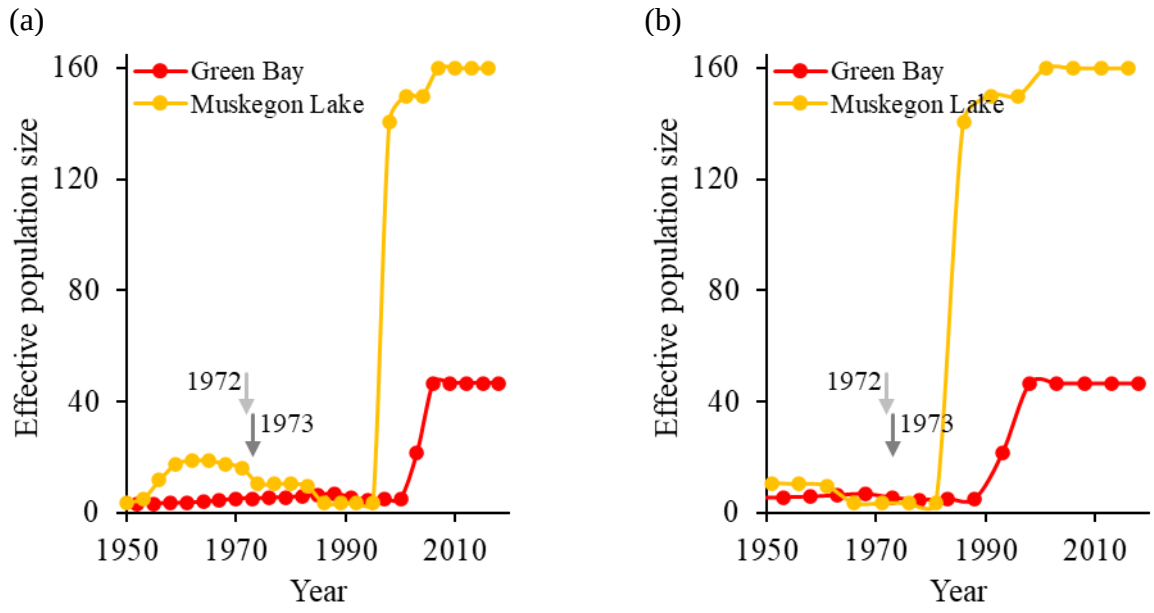

Supplementary Figure 10. Effective population sizes of Green Bay and Muskegon Lake before and after environmental remediation driven by environmental initiatives, such as the Clean Water Act since 1972 (indicated with a light gray arrow) and the Muskegon County advanced wastewater treatment since 1973 (indicated with a dark gray arrow). Given an estimated generation time of 3 (a) or 5 (b) years, the effective population sizes of yellow perch populations began rebounding approximately 10-30 years after clean-up efforts were under way.

Supplementary Table 1. Sampling information where we report the sample site name, the year and month in which sampling was conducted (sampling month is available for a subset of samples), the number of individuals sequenced, and the latitude and longitude (degree).

Sample site	Sample date	Sample size	Latitude	Longitude
Green Bay	2018 (May)	30	44.513332	-88.015831
Muskegon Lake	2016 (July)	30	43.224194	-86.235809
Grand Haven	2018	30	43.063073	-86.228386
Michigan City	2018 (May, June)	29	41.707539	-86.895030
Milwaukee	2018 (November), 2019 (May, June)	30	43.038902	-87.906471
Naubinway	2018	30	46.092497	-85.447597
Sutton’s Bay	2018 (June)	31	44.976666	-85.650639

Supplementary Table 2. Mapping quality of samples.

Sample ID	No. total reads	No. mapped reads	No. reads with mapping quality ≥ 20	No. reads with mapping quality ≥ 60
D9_320	68974612	68749732	62937577	57988746
D9_321	74566897	74351942	67920178	62324911
D9_322	67046756	66841947	61658345	56928066
D9_323_01	6641129	6624704	6095028	5614903
D9_323_02	65871425	65693206	60334194	55550578
D9_324_01	15211359	15168756	13877336	12725733
D9_324_02	55650616	55485192	50653463	46422030
D9_325	68281196	68073383	62133017	57036603
D9_326	73899079	73679379	67372931	61959692
D9_327	80464504	80157897	71445105	64967087
D9_328	77365549	77134390	70435287	64877972
D9_329	67774495	67555970	62287865	57544889
D9_330_01	6566099	6544459	5990365	5510866
D9_330_02	65534880	65300036	59647765	54830635
D9_331	67886493	67646208	62130041	57335329
D9_332	76423556	76195516	70378444	65088422
D9_333	72882737	72657501	66559265	61333697
D9_334	66618680	66432719	60884016	56013353
D9_335	68047077	67869904	62297028	57392000
D9_336	83353851	83108303	76491550	70484719
D9_337	70522338	70315012	65100977	60249553
D9_338	79973085	79760831	73614776	68004053
D9_339	99880285	99575820	91851878	84831527
D9_340	69603336	69398869	62949563	57517590
D9_341	68204357	68002230	62887494	58140145
D9_342	72957028	72740460	66847119	61551112
D9_343	85120740	84828815	76867347	70333007
D9_344_01	63201193	63028680	58089887	53543410
D9_344_02	7470224	7450340	6847199	6309619
D9_345	73593597	73384082	67378443	62050839
D9_346	67112446	66934763	61664982	56889246
D9_347	67550362	67382640	61606572	56543407
D9_348	80185861	79964261	73681463	68021652
D9_349	79121017	78922319	72621400	66994348
GBT18_1	68623479	68357250	61317646	55922454
GBT18_2_01	63692603	63491543	57758862	52877258
GBT18_2_02	7283936	7262243	6584599	6027384
GBT18_5	71119000	70693177	60855292	54432686
GBT18_6	70139708	69853831	61378131	55464634
GBT18_7	73787148	73531437	64150405	57812429
GBT18_8	84790813	84492446	76673301	69972318

GBT18_9_01	62327039	62138895	56549703	51789542
GBT18_9_01	9853830	9822696	8920447	8168135
GBT18_10_01	59318041	59115344	53839765	49337484
GBT18_10_02	12195698	12154728	11039034	10115936
GBT18_11	71910779	71659746	64183444	58483919
GBT18_12	69998187	69762886	63235807	57788229
GBT18_13	83743156	83378753	75970165	69584654
GBT18_14	69609065	69367539	63063025	57689296
GBT18_16	79846107	79588194	72660450	66677010
GBT18_18	77609825	77323320	70124655	64082735
GBT18_19	67033193	66780220	60583511	55427939
GBT18_20	86698500	86405263	78790592	72073647
GBT18_21	83699226	83434882	75964802	69479441
GBT18_24	87663824	87328045	79514753	72812469
GBT18_25	84133021	83871561	76826878	70454442
GBT18_26	80628626	80385665	73803392	67753037
GBT18_28	82991626	82681361	75308149	68969798
GBT18_29	98921913	98595327	89819103	82203138
GBT18_31	66323385	66082811	59922001	54709298
GBT18_32	81387684	81151006	73932707	67705258
GBT18_33	73966413	73737824	67358284	61728889
GBT18_34_01	6563900	6544615	5948063	5447558
GBT18_34_02	64581427	64380496	58819997	53850821
GBT18_35	72262119	72027236	66066040	60637058
GBU18_9	79845989	79592301	72729220	66601414
GBU18_17	84293767	83926951	76552734	70199378
GBU18_21	77260952	77033508	70742581	64944333
GH18_34	92815294	92432838	82966255	75637747
GH18_35	112245909	111807969	96312275	86307334
GH18_37	80292962	79989530	72075265	65773550
GH18_38	89934948	89572941	80461283	73345462
GH18_39	81837279	81511299	72327335	65789878
GH18_40	91154587	90799797	80655947	73175635
GH18_41	83616893	83288093	74338451	67466357
GH18_42	92119863	91756620	80182515	72382085
GH18_43	86487475	86230503	78664818	72096531
GH18_45	68327717	68133761	62460905	57368692
GH18_46	87349587	87040412	76251490	68859822
GH18_49	103021745	102644042	92718288	84746617
GH18_51	94632403	94256019	84343865	76837329
GH18_52_01	63082765	62909800	57356059	52622841
GH18_52_02	8153457	8130179	7396929	6787449
GH18_53	69689268	69481517	63584413	58406581
GH18_55	74391302	74167062	67446151	61875768

GH18_59	66861130	66608707	59756899	54502858
GH18_61	70713969	70493489	63812743	58420373
GH18_62_01	61065851	60875735	55119498	50471054
GH18_62_02	10712588	10680511	9632729	8820556
GH18_66_01	56515693	56338129	50590251	46190131
GH18_66_02	17922626	17863860	15994387	14604766
GH18_67_01	64293330	64126123	58618260	53839373
GH18_67_02	7825744	7804436	7117881	6538464
GH18_68_01	64125923	63954795	58299055	53458230
GH18_68_02	7588283	7566831	6884682	6315334
GH18_69_01	57734839	57584602	52870362	48675456
GH18_69_02	14565470	14529093	13298664	12245823
GH18_72	76129214	75895557	68677524	62904260
GH18_73	81252936	80981585	73424106	67287338
GH18_74	76255517	76033299	69116707	63328771
GH18_75	88361092	88082455	80366287	73736508
GH18_76_01	63413352	63236583	57785005	53050946
GH18_76_02	7227595	7207886	6565260	6028350
GH18_77	66332675	66120240	60075746	55077984
GH18_78	72591209	72340949	66063722	60712532
IMC18_1_01	18617370	18569369	16998507	15645898
IMC18_1_02	55278831	55110990	50452458	46375503
IMC18_2_01	17070294	17023866	15538016	14280882
IMC18_2_02	57290634	57111054	52153932	47862418
IMC18_3_01	7126210	7104053	6489538	5970024
IMC18_3_02	64220295	64009026	58519127	53804413
IMC18_4_01	18490974	18429434	16830355	15466064
IMC18_4_02	55625345	55420687	50642123	46488858
IMC18_5_01	13666175	13609602	12398797	11380809
IMC18_5_02	59592886	59333077	54059929	49557491
IMC18_9	62618757	62256742	56073835	51381234
IMC18_11	69134333	68925428	62865600	57720646
IMC18_12	66757172	66548733	60779596	55830716
IMC18_13	70557688	70309646	64734981	59664876
IMC18_14	87507395	87181933	79734680	73258660
IMC18_15_01	11060921	11027847	10089934	9289010
IMC18_15_02	60095852	59904375	54877126	50488353
IMC18_16_01	21952038	21881051	20035335	18455822
IMC18_16_02	55602530	55402915	50754831	46692788
IMC18_17_01	19909607	19835730	18136432	16676339
IMC18_17_02	55951133	55732486	50973535	46805545
IMC18_18_01	10037440	10006896	9163446	8430755
IMC18_18_02	59099424	58892076	53746330	49314590
IMC18_21	103323183	102928569	94050818	86418192

IMC18_23_01	7436899	7416515	6798459	6256744
IMC18_23_02	63290106	63098612	57920801	53283306
IMC18_25	64179701	63927853	58289957	53548291
IMC18_26_01	12556952	12519668	11411320	10496079
IMC18_26_02	59555667	59356177	54126396	49715706
IMC18_27_01	9351202	9321091	8504366	7811360
IMC18_27_02	62139194	61925544	56590872	51952975
IMC18_29_01	24093693	23959743	21898001	20127340
IMC18_29_02	54907530	54584201	49910168	45802646
IMC18_31_01	30919000	30832812	28188328	25920414
IMC18_31_02	47701681	47558762	43495280	39948407
IMC18_32_01	22483254	22424244	20454392	18806159
IMC18_32_02	52452787	52296065	47734216	43826410
IMC18_33	75278109	75031642	68583569	63022919
IMC18_34	67385961	67137791	61547840	56672256
IMC18_35	71051582	70755440	64362328	58958445
IMC18_36	66179763	65952595	60460508	55568395
IMC18_38	68378935	68095947	62448184	57434157
IMC18_42	71203271	70954102	64678786	59281151
IMC18_46_01	27827191	27736620	25230175	23174239
IMC18_46_02	54515330	54298731	49491132	45423594
MIL19_1_01	12873364	12834904	11678718	10717152
MIL19_1_02	61118042	60942408	55682792	51088355
MIL19_2_01	13098239	13059280	11924050	10968241
MIL19_2_02	60909342	60734113	55656382	51199904
MIL19_3	50669255	50437067	46051927	42313549
MIL19_4	57325235	57071088	51870372	47523379
MIL19_5_01	24028540	23927225	21940558	20230262
MIL19_5_02	52070621	51873050	47627892	43918625
MIL19_7	61372281	61122126	55684525	51025198
MIL19_8_01	5295395	5271370	4814533	4420101
MIL19_8_02	13989427	13919680	12738726	11683597
MIL19_8_03	51067368	50832125	46364474	42600546
MIL19_9_01	22593889	22522325	20461062	18783263
MIL19_9_02	55709144	55542789	50673507	46524052
MIL19_10_01	9890318	9853867	8961916	8184925
MIL19_10_02	61723892	61511921	55682814	50941908
MIL19_11_01	21520067	21460158	19540324	17941790
MIL19_11_02	56200400	56052596	51217405	47027484
MIL19_12_01	10621481	10578409	9651147	8815866
MIL19_12_02	61200635	60983353	55366888	50696567
MIL19_13	68473492	68253545	62133720	57045788
MIL19_14	68078088	67823040	61593518	56436432
MIL19_15	67964702	67724932	61547017	56408195

MIL19_16	62896023	62644658	56933216	52168651
MIL19_17_01	29996340	29908865	27298215	25075960
MIL19_17_02	48253884	48127301	43960404	40387854
MIL19_18_01	14492551	14451028	13119586	12029520
MIL19_18_02	59646990	59484183	54231849	49729751
MIL19_19	73849326	73565080	66887489	61339515
MIL19_20_01	19751856	19661864	17977105	16587452
MIL19_20_02	57162170	56916777	52324980	48274610
MIL19_21	81044909	80744308	73157257	66922528
MIL19_22_01	20191316	20115527	18475662	17064683
MIL19_22_02	57404553	57204250	52615173	48595190
MIL19_23_01	23094528	23005343	20792892	19063061
MIL19_23_02	55723416	55547894	50456987	46304208
MIL19_24	68299065	68053418	62122271	57053421
MIL19_25_01	20747592	20688390	18868951	17340726
MIL19_25_02	53331126	53183780	48718294	44771786
MIL19_26	82987299	82711208	75283713	69023519
MIL19_28	77925516	77687704	70921409	65189146
MIL19_29_01	14942243	14898160	13587071	12487443
MIL19_29_02	59902950	59732785	54633850	50230555
MIL19_30_01	9428785	9386854	8554239	7871047
MIL19_30_02	64322946	64041198	58629354	53938661
MIL19_31	74152218	73878776	67215784	61655134
MIL19_32_01	28214887	28108666	25622971	23601355
MIL19_32_02	46867350	46710082	42816031	39452256
MTC18_1_01	23564358	23492652	21547010	19855471
MTC18_1_02	56185420	55984799	51453321	47378834
MTC18_2_01	34982011	34854438	31875969	29351136
MTC18_2_02	45752089	45560721	41777376	38438739
MTC18_3_01	27227378	27144503	24955963	23022857
MTC18_3_02	50936139	50763740	46762542	43118451
MTC18_4_01	26007797	25912445	23624374	21716079
MTC18_4_02	55741612	55493255	50698153	46561311
MTC18_5	68309255	68025350	62529078	57754080
MTC18_6_01	15774182	15725016	14454408	13348649
MTC18_6_02	60489076	60271577	55512513	51219434
MTC18_7	59213857	59004085	53756457	49222522
MTC18_8_01	59458775	59264020	54233100	49889344
MTC18_8_02	11961165	11917990	10893406	10016685
MTC18_9	53711337	53257177	46997279	42341364
MTC18_10	59239264	59033356	53802182	49249641
MTC18_12_01	45435627	45292638	41239631	37810185
MTC18_12_02	29468528	29380218	26668097	24442731
MTC18_13	67837764	67066098	57589358	51949336

MTC18_14	64186647	62724203	54042596	48441091
MTC18_15_01	59052876	58851400	54183662	49961284
MTC18_15_02	12238213	12191168	11205575	10326776
MTC18_16	67564725	67280989	61429582	56422919
MTC18_17	60970531	60749268	55558460	50956835
MTC18_19	63651802	63366563	57203952	52365642
MTC18_20	47257075	47043232	42736760	39172213
MTC18_21	55107542	54880583	49674862	45484970
MTC18_22	63642397	63246839	57069180	52363083
MTC18_23	55470437	55305824	49297612	44650059
MTC18_24	67598217	66592441	59474710	54080208
MTC18_25	61631037	61127538	54180222	49152427
MTC18_26_01	55203224	55046689	50418073	46329599
MTC18_26_02	17306482	17250031	15775570	14489838
MTC18_27_01	65989265	65651398	60762470	56162584
MTC18_27_02	7590159	7548782	6978627	6447277
MTC18_28_01	52698437	52532049	48325159	44537055
MTC18_28_02	19880647	19808867	18179184	16741176
MTC18_29	75709649	75002250	65719249	59273469
MTC18_30	72520383	72290615	66651517	61449563
MTC18_32	70361708	70035421	63568510	58141852
MTC18_33	35006694	34865089	31650730	29016771
MTC18_34_01	55905618	55715528	50987730	46773939
MTC18_34_02	20574600	20506262	18715437	17159933
NUB18_3	71895809	71574712	64958022	59497283
NUB18_6	74480298	74178121	67585201	62018207
NUB18_8	73647600	71092733	64088134	58586861
NUB18_13	77617924	77321625	69950548	64053338
NUB18_15	72498700	71493666	64783187	59393370
NUB18_16	73883820	73651099	67115130	61564554
NUB18_19	75499786	75081179	68212938	62619515
NUB18_22	74760289	74541418	67240322	61464354
NUB18_25	80064998	79826711	71624858	65541320
NUB18_26	80820859	80490473	71577342	65325826
NUB18_27	70265632	70020567	62481235	56991755
NUB18_31	72461885	72174108	64192895	58496564
NUB18_34	77546827	77303975	69488464	63502039
NUB18_35	71882837	71636713	64447439	58984074
NUB18_39	67939040	67739689	60708195	55472141
NUB18_40	76747328	76543643	68787644	62932820
NUB18_41	70443379	70191165	63260834	57949128
NUB18_42_01	17345938	17255376	15541308	14227907
NUB18_42_02	59589156	59242775	53468985	48924522
NUB18_45_01	12547463	12498623	11387158	10473271

NUB18_45_02	62494347	62219498	56809960	52222840
NUB18_47_01	15359483	15317415	13794708	12627336
NUB18_47_02	61227711	61022135	55054237	50353359
NUB18_56	78847165	78314637	71205565	65308989
NUB18_58_01	17942146	17868407	16125369	14774803
NUB18_58_02	59292944	59008187	53359094	48843784
NUB18_59_01	15426933	15374751	13945177	12804303
NUB18_59_02	61033611	60793187	55239849	50695784
NUB18_62_01	25849203	25782512	23422051	21483486
NUB18_62_02	55108229	54941690	49981857	45816091
NUB18_63_01	10698326	10664547	9598341	8776564
NUB18_63_02	63940138	63697179	57434431	52459570
NUB18_66_01	25604437	25509222	22654762	20586503
NUB18_66_02	56026172	55778749	49678165	45111562
NUB18_67_01	14582071	14447995	12983481	11859884
NUB18_67_02	61463346	60851460	54789575	50005353
NUB18_69_01	14452177	14386651	13026014	11955777
NUB18_69_02	61517119	61202326	55535176	50934850
NUB18_70_01	16474123	16425475	14840161	13595306
NUB18_70_02	60568179	60357073	54654999	50041803
NUB18_72_01	22827761	22736342	20453140	18704977
NUB18_72_02	53467886	53224811	47977083	43824861

Supplementary Table 3. Data sets of SNPs for population genetic and demographic analyses where we report the specific analysis for which different data sets were used and how the corresponding results are illustrated.

Data sets of SNPs	Analysis	Results
Study-wide data set	Phylogenetic tree construction	Fig. 1b Supplementary Fig. 1
Study-wide data set	Principal coordinate analysis	Fig. 1c Supplementary Fig. 2 Supplementary Fig. 3
Study-wide data set	Admixture analysis	Fig. 1d Supplementary Fig. 4
Within-group data set	Comparison of numbers of SNPs	Fig. 2a
Within-group data set	Comparison of minor allele frequency across sample sites	Fig. 2b
Within-group data set	Tajima's D calculation (MAF $\geq$ 0.02)	Fig. 2c
Within-group data set	Effective population size estimated by NeEstimator V2	Fig. 3a
Within-group data set	Genetic diversity calculation	Fig. 3c Supplementary Fig. 5
Within-group data set	Demographic history reconstructed by GONE	Fig. 3d Fig. 3e Supplementary Fig. 6

Supplementary Table 4. Numbers of single nucleotide polymorphisms (SNPs) out of Hardy-Weinberg equilibrium (HWE) in the within-group data set (MAF ≥ 0.05). A SNP is detected as out of HWE when its *P* value, calculated using VCFtools (0.1.16)(37), is smaller than the Bonferroni-corrected significance level at α=0.05 (*i.e.*, 0.05 divided by the total number of SNPs being tested).

Population	No. SNPs being tested	No. SNPs out of HWE
Green Bay	2,186,762	4,725
Muskegon Lake	2,275,931	4,548
Grand Haven	670,575	5,724
Michigan City	775,907	6,920
Milwaukee	776,082	6,186
Naubinway	711,223	5,877
Sutton's Bay	727,014	3,725

Supplementary Table 5. Mean Weir and Cockerham's F_{ST} between pairs of sample sites.

	Green Bay	Muskegon Lake	Grand Haven	Michigan City	Milwaukee	Naubinway
Muskegon Lake	0.051997					
Grand Haven	0.066478	0.058973				
Michigan City	0.066747	0.059198	0.000195			
Milwaukee	0.063981	0.056034	0.000324	-0.000186		
Naubinway	0.059522	0.051000	0.000558	0.001302	0.000585	
Sutton's Bay	0.054967	0.046033	0.004133	0.003823	0.003257	0.001339

Supplementary Table 6. Sequencing depth of all samples in all sample sites.

Population	Sample	Sequencing depth
Green Bay	GBT1801	11.51
Green Bay	GBT1802	11.97
Green Bay	GBT1805	11.85
Green Bay	GBT1806	11.74
Green Bay	GBT1807	12.31
Green Bay	GBT1808	14.25
Green Bay	GBT1809	12.2
Green Bay	GBT1810	12.08
Green Bay	GBT1811	12.08
Green Bay	GBT1812	11.85
Green Bay	GBT1813	14.13
Green Bay	GBT1814	11.74
Green Bay	GBT1816	13.45
Green Bay	GBT1818	13.11
Green Bay	GBT1819	11.28
Green Bay	GBT1820	14.59
Green Bay	GBT1821	14.13
Green Bay	GBT1824	14.82
Green Bay	GBT1825	14.25
Green Bay	GBT1826	13.68
Green Bay	GBT1828	14.02
Green Bay	GBT1829	16.64
Green Bay	GBT1831	11.17
Green Bay	GBT1832	13.68
Green Bay	GBT1833	12.54
Green Bay	GBT1834	11.97
Green Bay	GBT1835	12.2
Green Bay	GBU1809	13.45
Green Bay	GBU1817	14.25
Green Bay	GBU1821	13.11
Muskegon Lake	D9320	11.63
Muskegon Lake	D9321	12.54
Muskegon Lake	D9322	11.28
Muskegon Lake	D9323	12.2
Muskegon Lake	D9324	11.97
Muskegon Lake	D9325	11.51
Muskegon Lake	D9326	12.42
Muskegon Lake	D9327	13.45
Muskegon Lake	D9328	12.99
Muskegon Lake	D9329	11.4
Muskegon Lake	D9330	12.2
Muskegon Lake	D9331	11.4

Muskegon Lake	D9332	12.88
Muskegon Lake	D9333	12.31
Muskegon Lake	D9334	11.28
Muskegon Lake	D9335	11.51
Muskegon Lake	D9336	14.13
Muskegon Lake	D9337	11.85
Muskegon Lake	D9338	13.45
Muskegon Lake	D9339	16.87
Muskegon Lake	D9340	11.74
Muskegon Lake	D9341	11.51
Muskegon Lake	D9342	12.31
Muskegon Lake	D9343	14.36
Muskegon Lake	D9344	11.97
Muskegon Lake	D9345	12.42
Muskegon Lake	D9346	11.28
Muskegon Lake	D9347	11.4
Muskegon Lake	D9348	13.56
Muskegon Lake	D9349	13.33
Grand Haven	GH1834	15.61
Grand Haven	GH1835	18.58
Grand Haven	GH1837	13.45
Grand Haven	GH1838	15.16
Grand Haven	GH1839	13.68
Grand Haven	GH1840	15.27
Grand Haven	GH1841	14.02
Grand Haven	GH1842	15.27
Grand Haven	GH1843	14.59
Grand Haven	GH1845	11.51
Grand Haven	GH1846	14.47
Grand Haven	GH1849	17.32
Grand Haven	GH1851	15.84
Grand Haven	GH1852	11.97
Grand Haven	GH1853	11.74
Grand Haven	GH1855	12.54
Grand Haven	GH1859	11.28
Grand Haven	GH1861	11.85
Grand Haven	GH1862	12.08
Grand Haven	GH1866	12.54
Grand Haven	GH1867	12.2
Grand Haven	GH1868	12.08
Grand Haven	GH1869	12.2
Grand Haven	GH1872	12.88
Grand Haven	GH1873	13.68
Grand Haven	GH1874	12.88
Grand Haven	GH1875	14.93

Grand Haven	GH1876	11.97
Grand Haven	GH1877	11.17
Grand Haven	GH1878	12.31
Michigan City	IMC1801	12.42
Michigan City	IMC1802	12.54
Michigan City	IMC1803	12.08
Michigan City	IMC1804	12.54
Michigan City	IMC1805	12.31
Michigan City	IMC1809	10.49
Michigan City	IMC1811	11.63
Michigan City	IMC1812	11.28
Michigan City	IMC1813	11.97
Michigan City	IMC1814	14.7
Michigan City	IMC1815	11.97
Michigan City	IMC1816	13.11
Michigan City	IMC1817	12.76
Michigan City	IMC1818	11.63
Michigan City	IMC1821	17.44
Michigan City	IMC1823	11.97
Michigan City	IMC1825	10.83
Michigan City	IMC1826	12.2
Michigan City	IMC1827	12.08
Michigan City	IMC1829	13.33
Michigan City	IMC1831	13.22
Michigan City	IMC1832	12.65
Michigan City	IMC1833	12.65
Michigan City	IMC1834	11.4
Michigan City	IMC1835	11.97
Michigan City	IMC1836	11.17
Michigan City	IMC1838	11.51
Michigan City	IMC1842	12.08
Michigan City	IMC1846	13.9
Milwaukee	MIL1901	12.54
Milwaukee	MIL1902	12.54
Milwaukee	MIL1903	8.55
Milwaukee	MIL1904	9.69
Milwaukee	MIL1905	12.88
Milwaukee	MIL1907	10.37
Milwaukee	MIL1908	11.85
Milwaukee	MIL1909	13.22
Milwaukee	MIL1910	12.08
Milwaukee	MIL1911	13.11
Milwaukee	MIL1912	12.08
Milwaukee	MIL1913	11.51
Milwaukee	MIL1914	11.51

Milwaukee	MIL1915	11.4
Milwaukee	MIL1916	10.6
Milwaukee	MIL1917	13.22
Milwaukee	MIL1918	12.54
Milwaukee	MIL1919	12.42
Milwaukee	MIL1920	12.99
Milwaukee	MIL1921	13.68
Milwaukee	MIL1922	13.11
Milwaukee	MIL1923	13.22
Milwaukee	MIL1924	11.51
Milwaukee	MIL1925	12.54
Milwaukee	MIL1926	14.02
Milwaukee	MIL1928	13.11
Milwaukee	MIL1929	12.65
Milwaukee	MIL1930	12.42
Milwaukee	MIL1931	12.54
Milwaukee	MIL1932	12.65
Naubinway	NUB1803	12.08
Naubinway	NUB1806	12.54
Naubinway	NUB1808	12.42
Naubinway	NUB1813	13.11
Naubinway	NUB1815	12.2
Naubinway	NUB1816	12.42
Naubinway	NUB1819	12.65
Naubinway	NUB1822	12.54
Naubinway	NUB1825	13.45
Naubinway	NUB1826	13.56
Naubinway	NUB1827	11.74
Naubinway	NUB1831	12.2
Naubinway	NUB1834	12.99
Naubinway	NUB1835	12.08
Naubinway	NUB1839	11.4
Naubinway	NUB1840	12.88
Naubinway	NUB1841	11.85
Naubinway	NUB1842	12.99
Naubinway	NUB1845	12.65
Naubinway	NUB1847	12.88
Naubinway	NUB1856	13.33
Naubinway	NUB1858	12.99
Naubinway	NUB1859	12.88
Naubinway	NUB1862	13.68
Naubinway	NUB1863	12.54
Naubinway	NUB1866	13.68
Naubinway	NUB1867	12.76
Naubinway	NUB1869	12.76

Naubinway	NUB1870	12.99
Naubinway	NUB1872	12.88
Sutton’s Bay	MTC1801	13.45
Sutton’s Bay	MTC1802	13.56
Sutton’s Bay	MTC1803	13.22
Sutton’s Bay	MTC1804	13.79
Sutton’s Bay	MTC1805	11.51
Sutton’s Bay	MTC1806	12.88
Sutton’s Bay	MTC1807	10.03
Sutton’s Bay	MTC1808	12.08
Sutton’s Bay	MTC1809	9
Sutton’s Bay	MTC1810	10.03
Sutton’s Bay	MTC1812	12.65
Sutton’s Bay	MTC1813	11.28
Sutton’s Bay	MTC1814	10.71
Sutton’s Bay	MTC1815	12.08
Sutton’s Bay	MTC1816	11.4
Sutton’s Bay	MTC1817	10.26
Sutton’s Bay	MTC1819	10.71
Sutton’s Bay	MTC1820	7.98
Sutton’s Bay	MTC1821	9.23
Sutton’s Bay	MTC1822	10.71
Sutton’s Bay	MTC1823	9.35
Sutton’s Bay	MTC1824	11.4
Sutton’s Bay	MTC1825	10.37
Sutton’s Bay	MTC1826	12.2
Sutton’s Bay	MTC1827	12.42
Sutton’s Bay	MTC1828	12.2
Sutton’s Bay	MTC1829	12.65
Sutton’s Bay	MTC1830	12.2
Sutton’s Bay	MTC1832	11.85
Sutton’s Bay	MTC1833	5.93
Sutton’s Bay	MTC1834	12.88

Supplementary Table 7. Mean read depth of all samples in all sample sites as calculated from the within-group data sets (see "Variant calling and filtering" in Supplementary Materials for details).

Population	Sample	Mean read depth
Green Bay	GBT181	10.06
Green Bay	GBT1810	9.99
Green Bay	GBT1811	10.18
Green Bay	GBT1812	9.52
Green Bay	GBT1813	11.12
Green Bay	GBT1814	9.38
Green Bay	GBT1816	10.7
Green Bay	GBT1818	10.43
Green Bay	GBT1819	9.16
Green Bay	GBT182	9.83
Green Bay	GBT1820	11.67
Green Bay	GBT1821	11.34
Green Bay	GBT1824	12.16
Green Bay	GBT1825	11.48
Green Bay	GBT1826	11.18
Green Bay	GBT1828	11.94
Green Bay	GBT1829	13.12
Green Bay	GBT1831	9.5
Green Bay	GBT1832	11.17
Green Bay	GBT1833	10.33
Green Bay	GBT1834	9.72
Green Bay	GBT1835	9.81
Green Bay	GBT185	9.57
Green Bay	GBT186	9.5
Green Bay	GBT187	9.99
Green Bay	GBT188	11.17
Green Bay	GBT189	10.27
Green Bay	GBU1817	12.3
Green Bay	GBU1821	10.65
Green Bay	GBU189	10.97
Muskegon Lake	D9320	9.91
Muskegon Lake	D9321	10.4
Muskegon Lake	D9322	9.59
Muskegon Lake	D9323	10.2
Muskegon Lake	D9324	10.35
Muskegon Lake	D9325	9.59
Muskegon Lake	D9326	10.3
Muskegon Lake	D9327	11.84
Muskegon Lake	D9328	11.13

Muskegon Lake	D9329	9.56
Muskegon Lake	D9330	10.38
Muskegon Lake	D9331	9.72
Muskegon Lake	D9332	10.75
Muskegon Lake	D9333	10.62
Muskegon Lake	D9334	9.76
Muskegon Lake	D9335	9.48
Muskegon Lake	D9336	11.32
Muskegon Lake	D9337	9.5
Muskegon Lake	D9338	10.85
Muskegon Lake	D9339	13.58
Muskegon Lake	D9340	9.71
Muskegon Lake	D9341	9.56
Muskegon Lake	D9342	10.22
Muskegon Lake	D9343	11.82
Muskegon Lake	D9344	9.83
Muskegon Lake	D9345	9.87
Muskegon Lake	D9346	9.31
Muskegon Lake	D9347	9.47
Muskegon Lake	D9348	10.93
Muskegon Lake	D9349	10.81
Grand Haven	GH1834	14.76
Grand Haven	GH1835	16.1
Grand Haven	GH1837	13.25
Grand Haven	GH1838	14.45
Grand Haven	GH1839	12.84
Grand Haven	GH1840	14.62
Grand Haven	GH1841	13.54
Grand Haven	GH1842	14.35
Grand Haven	GH1843	13.37
Grand Haven	GH1845	11.01
Grand Haven	GH1846	13.12
Grand Haven	GH1849	16.74
Grand Haven	GH1851	15.34
Grand Haven	GH1852	11.29
Grand Haven	GH1853	11.31
Grand Haven	GH1855	11.77
Grand Haven	GH1859	10.92
Grand Haven	GH1861	11.71
Grand Haven	GH1862	11.69
Grand Haven	GH1866	12.72
Grand Haven	GH1867	11.78
Grand Haven	GH1868	11.22
Grand Haven	GH1869	11.69

Grand Haven	GH1872	12.21
Grand Haven	GH1873	12.98
Grand Haven	GH1874	12.41
Grand Haven	GH1875	13.88
Grand Haven	GH1876	11.2
Grand Haven	GH1877	10.87
Grand Haven	GH1878	11.7
Michigan City	IMC181	12.46
Michigan City	IMC1811	11.06
Michigan City	IMC1812	11.17
Michigan City	IMC1813	11.58
Michigan City	IMC1814	14.02
Michigan City	IMC1815	11.78
Michigan City	IMC1816	12.78
Michigan City	IMC1817	12.85
Michigan City	IMC1818	11.48
Michigan City	IMC182	12.33
Michigan City	IMC1821	15.9
Michigan City	IMC1823	11.86
Michigan City	IMC1825	10.11
Michigan City	IMC1826	12.17
Michigan City	IMC1827	11.76
Michigan City	IMC1829	13.1
Michigan City	IMC183	11.75
Michigan City	IMC1831	13.18
Michigan City	IMC1832	12.45
Michigan City	IMC1833	11.85
Michigan City	IMC1834	10.25
Michigan City	IMC1835	11.26
Michigan City	IMC1836	11.48
Michigan City	IMC1838	11.61
Michigan City	IMC184	12.24
Michigan City	IMC1842	12.08
Michigan City	IMC1846	14.42
Michigan City	IMC185	11.95
Michigan City	IMC189	9.97
Milwaukee	MIL191	12.63
Milwaukee	MIL1910	11.25
Milwaukee	MIL1911	12.92
Milwaukee	MIL1912	11.72
Milwaukee	MIL1913	10.91
Milwaukee	MIL1914	10.96
Milwaukee	MIL1915	10.91
Milwaukee	MIL1916	10.21

Milwaukee	MIL1917	13.33
Milwaukee	MIL1918	12.55
Milwaukee	MIL1919	11.46
Milwaukee	MIL192	12.38
Milwaukee	MIL1920	13.06
Milwaukee	MIL1921	13.08
Milwaukee	MIL1922	13.4
Milwaukee	MIL1923	13.23
Milwaukee	MIL1924	10.97
Milwaukee	MIL1925	12.41
Milwaukee	MIL1926	13.24
Milwaukee	MIL1928	12.39
Milwaukee	MIL1929	12.56
Milwaukee	MIL193	8.88
Milwaukee	MIL1930	12.22
Milwaukee	MIL1931	10.83
Milwaukee	MIL1932	13.14
Milwaukee	MIL194	8.5
Milwaukee	MIL195	13.31
Milwaukee	MIL197	9.64
Milwaukee	MIL198	11.76
Milwaukee	MIL199	12.94
Naubinway	NUB1813	12.07
Naubinway	NUB1815	11.39
Naubinway	NUB1816	11.92
Naubinway	NUB1819	12.26
Naubinway	NUB1822	12.45
Naubinway	NUB1825	12.73
Naubinway	NUB1826	13.03
Naubinway	NUB1827	11.42
Naubinway	NUB183	11.41
Naubinway	NUB1831	11.97
Naubinway	NUB1834	12.71
Naubinway	NUB1835	11.94
Naubinway	NUB1839	11.4
Naubinway	NUB1840	12.62
Naubinway	NUB1841	12.06
Naubinway	NUB1842	13.33
Naubinway	NUB1845	13.15
Naubinway	NUB1847	12.39
Naubinway	NUB1856	12.44
Naubinway	NUB1858	13.63
Naubinway	NUB1859	13.2
Naubinway	NUB186	11.8

Naubinway	NUB1862	13.47
Naubinway	NUB1863	13
Naubinway	NUB1866	13.87
Naubinway	NUB1867	13.07
Naubinway	NUB1869	13.36
Naubinway	NUB1870	13.39
Naubinway	NUB1872	13.3
Naubinway	NUB188	11.21
Sutton’s Bay	MTC181	13.29
Sutton’s Bay	MTC1810	9.5
Sutton’s Bay	MTC1812	12.04
Sutton’s Bay	MTC1813	9.42
Sutton’s Bay	MTC1814	9.09
Sutton’s Bay	MTC1815	10.94
Sutton’s Bay	MTC1816	10.35
Sutton’s Bay	MTC1817	7.17
Sutton’s Bay	MTC1819	9.94
Sutton’s Bay	MTC182	13.7
Sutton’s Bay	MTC1820	7.9
Sutton’s Bay	MTC1821	8.86
Sutton’s Bay	MTC1822	9.6
Sutton’s Bay	MTC1823	9.18
Sutton’s Bay	MTC1824	9.95
Sutton’s Bay	MTC1825	9.42
Sutton’s Bay	MTC1826	11.41
Sutton’s Bay	MTC1827	11.34
Sutton’s Bay	MTC1828	11.67
Sutton’s Bay	MTC1829	10.97
Sutton’s Bay	MTC183	13.15
Sutton’s Bay	MTC1830	11.29
Sutton’s Bay	MTC1832	8.09
Sutton’s Bay	MTC1833	6.04
Sutton’s Bay	MTC1834	12.85
Sutton’s Bay	MTC184	13.74
Sutton’s Bay	MTC185	11.5
Sutton’s Bay	MTC186	12.78
Sutton’s Bay	MTC187	6.05
Sutton’s Bay	MTC188	10.89
Sutton’s Bay	MTC189	8.27

Supplementary Table 8. Genomic positions of, numbers of SNPs on, and numbers of SNPs with $F_{ST} \geq 0.6$ on 13 outlier windows.

Outlier window	Chromosome	Start position	End position	No. SNPs	No. SNPs with $F_{ST} \geq 0.6$
1	1	2426937	2785691	3203	320
2	1	3544209	3739267	2290	163
3	1	15957452	16004538	363	141
4	4	34762415	34852528	2410	352
5	8	15887228	15918438	529	144
6	11	20466095	20615608	540	82
7	12	18929507	19043907	1173	184
8	13	21639613	21841952	1200	322
9	14	26911329	26930065	1265	194
10	18	14025882	14294333	1517	360
11	18	14911469	14941999	669	186
12	24	9892333	10102303	951	294
13	24	18658693	18978485	2449	190